

3 The Precambrian paleogeography of Laurentia

Nicholas L. Swanson-Hysell¹

¹ Department of Earth and Planetary Science, University of California, Berkeley, CA 94720 USA

This chapter is in preparation for the book Ancient Supercontinents and the Paleogeography of the Earth

¹ 3.1 Abstract

Laurentia was a major continent throughout the majority of the Proterozoic. It is hypothesized to have had a central position in both the Paleoproterozoic Nuna and Neoproterozoic Rodinia supercontinents. The paleogeographic position of Laurentia is key to the development of reconstructions of Proterozoic paleogeography. There is a rich record of Precambrian paleomagnetic poles from Laurentia, as well as an extensive and well-documented geologic history of tectonism. These geologic and paleomagnetic records are increasingly better constrained geochronologically and are both key to evaluating and developing paleogeographic models. Data from the Slave and Superior provinces of Laurentia provide what is arguably the strongest evidence of differential plate tectonics in the Rhyacian and Orosirian Periods of the Paleoproterozoic Era (2.3 to 1.8 Ga) leading up to the collision of these terranes during the Trans-Hudson orogeny. The collisions of these and other Archean provinces led to the formation of the core of Laurentia. Subsequent crustal growth occurred through multiple intervals of accretionary orogenesis through the late Paleoproterozoic and Mesoproterozoic until the continent-continent collision of the Grenvillian orogeny that was ongoing at the Mesoproterozoic-Neoproterozoic boundary (1.0 Ga). The lead-up to this orogeny was associated with rapid plate motion of Laurentia from high latitudes towards the equator recorded by the Logan Loop and Keweenawan Track of paleomagnetic poles. Following, a return to high-latitudes as constrained by paleomagnetic poles of the Grenville Loop, Laurentia straddled the equator at the time of Cryogenian Snowball Earth glaciation as part of the Rodinia supercontinent. Rifting and passive margin development then isolated Laurentia in the early Paleozoic Era. Subsequent

22 accretionary and collisional orogenesis occurred associated with the Appalachian orogenic cycle
23 with Laurentia first colliding with Avalonia–Baltica to become Laurussia and Laurussia then
24 uniting with Gondwana to form Pangea. While the details of the conjugate continents are better
25 reconstructed for this last Wilson cycle, the broad features of the Trans-Hudson, Grenvillian and
26 Appalachian orogenic cycles bear similarities. In each case, accretionary collision of arc terranes
27 was followed by continent-continent collision. The major difference is that the collisions of the
28 Grenvillian and Appalachian orogenic cycles resulted in relatively minor crustal growth compared
29 to the Trans-Hudson. Break-up following the Grenvillian and Appalachian orogenic cycles
30 occurred along the same margin as collision while the major orogens of the Trans-Hudson
31 orogenic cycle have remained sutured. As a result, Laurentia has been a formidable continent for
32 the past 1.8 billion years whose position and history is key for reconstructing global
33 paleogeography. The evidence from Laurentia provides strong-support for mobile lid plate
34 tectonic processes operating over the past 2.2 billion years.

35 **3.2 Introduction and broad tectonic history**

36 Laurentia refers to the craton that forms the Precambrian core of North America (Fig. 1).
37 Laurentia is comprised of multiple Archean provinces that had unique histories prior to their
38 amalgamation in the Paleoproterozoic, as well as tectonic zones of crustal growth that post-date
39 this assembly (Hoffman, 1989; Whitmeyer and Karlstrom, 2007). Collision between the Superior
40 province and the composite Slave+Rae+Hearne provinces that resulted in the Trans-Hudson
41 orogeny represents a major event in the formation of Laurentia (Corrigan et al., 2009). Terminal
42 collision recorded in the Trans-Hudson orogen is estimated to have been ca. 1.86 to 1.82 Ga based
43 on constraints such as U-Pb dating of monazite grains and zircon rims (Skipton et al., 2016;
44 Weller and St-Onge, 2017, e.g.). A period of accretionary and collision orogenesis is recorded in
45 the constituent provinces and terranes of Laurentia leading up to the terminal collision of the
46 Trans-Hudson orogeny. This overall story of rapid Paleoproterozoic amalgamation of Laurentia's
47 constituent Archean provinces, including the terminal Trans-Hudson orogeny, was synthesized in
48 the seminal *United Plates of America* paper of Hoffman (1988) and has been refined in the time
49 since – particularly with additional geochronological constraints. Of most relevance here are the

50 events that led to the suturing of more major Archean provinces: the Thelon orogen associated
51 with the collision between the Slave and Rae provinces ca. 2.0 to 1.9 Ga (Hoffman, 1989); the
52 Snowbird orogen associated with ca. 1.89 Ga collision between the Rae and Hearne provinces and
53 associated terranes (Berman et al., 2007); the Nagssugtoqidian orogen due to the ca. 1.86 to 1.84
54 Ga collision between the Rae and North Atlantic provinces (St-Onge et al., 2009); and the
55 Torngat orogen resulting from the ca. 1.87 to 1.85 Ga collision of the Meta Incognita province
56 (grouped with the Rae province in older compilations) with the North Atlantic province (St-Onge
57 et al., 2009). As for the Wyoming province, many models posit that it was conjoined with Hearne
58 and associated provinces at the time of the Trans-Hudson orogeny (e.g. St-Onge et al., 2009;
59 Pehrsson et al., 2015) or was proximal to Hearne and Superior while still undergoing continued
60 translation up to ca. 1.80 Ga (Whitmeyer and Karlstrom, 2007). A contrasting view has been
61 been proposed that the Wyoming province and Medicine Hat blocks was not conjoined with the
62 other Laurentia provinces until ca. 1.72 Ga (Kilian et al., 2016). This interpretation is argued to
63 be consistent with geochronological constraints on monazite and metamorphic zircon indicating
64 active collisional orogenesis associated with the Big Sky orogen on the northern margin of the
65 craton as late as ca. 1.75 to 1.72 Ga (Condit et al., 2015) and ca. 1.72 tectonomagmatic activity
66 in the Black Hills region (Redden et al., 1990). However, the evidence for earlier orogenesis ca.
67 1.78 to 1.75 in the Black Hills (Dahl et al., 1999; Hrncir et al., 2017), as well as high-grade
68 tectonism as early as ca. 1.81 Ga in the Big Sky orogen (Condit et al., 2015), may support the
69 interpretation of Hrncir et al. (2017) that ca. 1.72 Ga activity is a minor overprint on ca. 1.75
70 terminal suturing between Wyoming and Superior. Regardless, in both of these interpretations,
71 Wyoming is a later addition to Laurentia with final suturing post-dating ca. 1.82 Ga
72 amalgamation of Archean provinces with the Trans-Hudson orogen further to the northeast.
73 Overall, the collision of these Archean microcontinents between ca. 1.9 and 1.8 Ga lead to rapid
74 amalgamation of the majority of the Laurentia craton.

75 Crustal growth also progressed in the Paleoproterozoic through accretionary orogenesis. This
76 accretion occurred within the Wopmay orogen through ca. 1.88 Ga arc-continent collision that led
77 to the accretion of the Hottah terrane (the Calderian orogeny) and the subsequent emplacement
78 of the Great Bear magmatic zone from ca. 1.88 to 1.84 Ga (Hildebrand et al., 2009). Coeval with

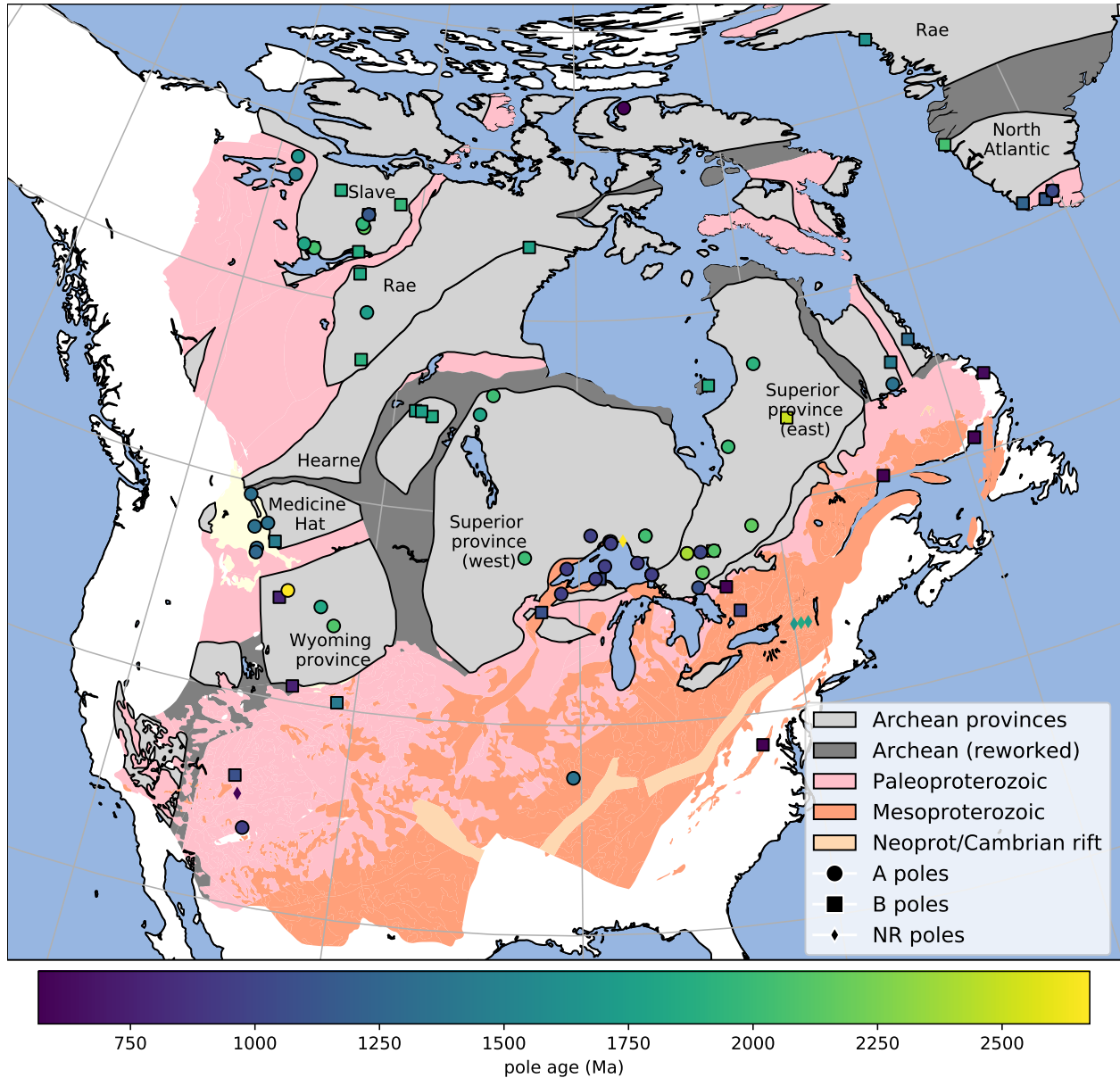


Figure 1. Simplified map of Laurentia showing the location of Archean provinces (labeled with text) and younger Paleoproterozoic and Mesoproterozoic crust (simplified from Whitmeyer and Karlstrom, 2007 with additions for Greenland based on St-Onge et al., 2009). The localities from which the compiled Precambrian paleomagnetic poles were developed are shown and colored by age. The circles (A rated poles) and squares (B rated poles) have been assessed by the Nordic workshop panel.

79 the Trans-Hudson orogeny was the peripheral Penokean orogeny during which both microcontinent
80 blocks (the Marshfield terrane) and arc terranes accreted on the southeastern margin of the west
81 Superior province ca. 1.86 to 1.82 (Schulz and Cannon, 2007). Firm evidence of the end of the
82 orogeny comes from the ca. 1.78 undeformed plutons of the post-Penokean East Central
83 Minnesota Batholith (Holm et al., 2005).

84 In the paleogeographic model framework of Pehrsson et al. (2015), the collisions of provinces
85 and terranes leading up to the Trans-Hudson orogeny mark the initial phase of assembly of the
86 supercontinent Nuna. The Trans-Hudson orogeny itself is taken to be the terminal collision
87 associated with the closure of the Manikewan Ocean that had previously been a large oceanic tract
88 separating the Superior province from the composite Slave+Rae+Hearne+North Atlantic
89 provinces (often referred to as the Churchill domain or plate; e.g. Skipton et al., 2016; Weller and
90 St-Onge, 2017). The Pehrsson et al. (2015) model posits that this period terminal collision not
91 only resulted in the amalgamation of Laurentia, but is also associated with the assembly of the
92 supercontinent Nuna that is hypothesized to include other major Paleoproterozoic cratons
93 including Siberia, Congo/São Francisco, West Africa, and Amazonia (Whitmeyer and Karlstrom,
94 2007; Pehrsson et al., 2015).

95 Following the Trans-Hudson orogeny, the locus of orogenesis migrated to the exterior of
96 Laurentia. This change marks a shift in the predominant style of Laurentia's growth as subsequent
97 crustal growth occurred dominantly through accretion of juvenile crust along the southern and
98 eastern margin of the nucleus of Archean provinces (Whitmeyer and Karlstrom, 2007; Figs. 1 and
99 2). Determining the extent of these belts is complicated by poor exposure of them in the
100 midcontinent relative to the exposure of the Archean provinces throughout the Canadian shield.
101 Major growth of Laurentia following the amalgamation of these Archean provinces occurred
102 associated with the arc-continent collision of the ca. 1.71 to 1.68 Ga Yavapai orogeny. Yavapai
103 orogenesis is interpreted to have resulted from the accretion of a series of arc terranes that
104 collided with each other and Laurentia (Karlstrom et al., 2001). Yavapai accretion was followed
105 by widespread emplacement of granitoid intrusions (Whitmeyer and Karlstrom, 2007). These
106 intrusions are hypothesized to have stabilized the juvenile accreted terranes that subsequently
107 remained part of Laurentia (Whitmeyer and Karlstrom, 2007). Subsequent accretionary

108 orogenesis of the ca. 1.65–1.60 Ga Mazatzal Orogeny and associated plutonism lead to further
109 crustal growth in the latest Paleoproterozoic (Karlstrom and Bowring, 1988). Laurentia's growth
110 continued in the Mesoproterozoic along the southeast margin through further juvenile terrane and
111 arc accretion. An interval of major plutonism occurred ca. 1.48–1.35 Ga leading to the formation
112 of A-type granitoids throughout both Mesoproterozoic and Paleoproterozoic provinces extending
113 from the southwest United States up to the Central Gneiss Belt of Ontario to the northeast of
114 Georgian Bay (Slagstad et al., 2009). This plutonism is likely due to crustal melting within a
115 back-arc region of ca. 1.50 to 1.43 Ga accretionary orogenesis (Bickford et al., 2015). Younger
116 magmatic activity ca. 1.37 Ga of the Southern Granite–Rhyolite Province suggests a similar
117 tectonic setting of accretionary orogenesis at that time (Bickford et al., 2015). While an active
118 margin interpretation with magmatism in back-arc setting has gained traction within the
119 literature with additional data, the tectonic setting is often described as enigmatic given earlier
120 interpretations of an anorogenic setting (see references in Slagstad et al., 2009).

121 Accretionary orogenesis continued along the (south)east margin of Laurentia with the
122 arc-continent collision of the ca. 1.25-1.22 Ga Elzevirian orogeny (McLelland et al., 2013). The
123 subsequent ca. 1.19 to 1.16 Ga Shawinigan orogeny is interpreted to be due to the accretion of a
124 terrane comprised of amalgamated arc volcanics and associated metasediments and is followed by
125 a period of tectonic quiescence on the eastern margin of Laurentia until the collision orogenesis of
126 the Grenvillian orogeny (McLelland et al., 2010). In the latest Mesoproterozoic (ca. 1.11-1.08
127 Ga), a major intracontinental rift co-located with a large igneous province formed in Laurentia's
128 interior leading to extension within the Archean Superior province and Paleoproterozoic
129 provinces. This Midcontinent Rift lead to the formation of a thick succession of volcanics and
130 mafic intrusions that are well-preserved in Laurentia's interior. Midcontinent Rift development
131 ceased as major collisional orogenesis of the Grenvillian orogeny began (Swanson-Hysell et al.,
132 2019). The Grenvillian orogeny was a protracted interval of continent-continent collision (ca. 1.09
133 to 0.98 Ga) leading to amphibolite to granulite facies metamorphism through the orogen
134 (McLelland et al., 2010). The orogeny is interpreted to have resulted in the development of a
135 thick orogenic plateau (Rivers, 2008).

136 There is significantly less preserved crustal growth on the western margin of Laurentia (Fig. 1)

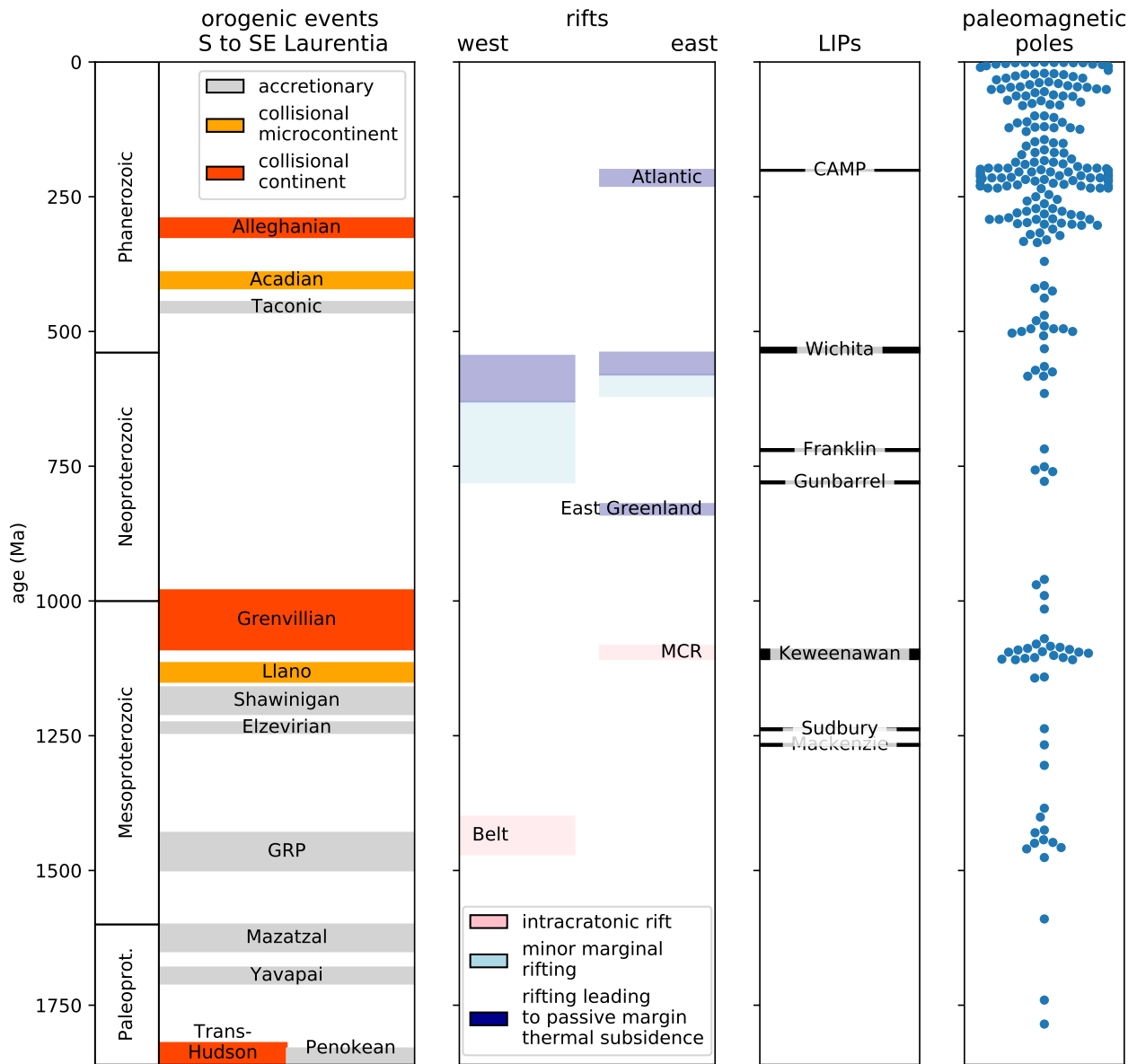


Figure 2. Simplified timeline of Laurentia's tectonic history over the past ~1.8 billion years. Brief summaries and references related to the orogenic and rifting episodes are given in the text. A timeline of large igneous provinces (LIPs) associated with typically brief and voluminous (or interpreted to be voluminous) volcanism is also shown. The interpreted age of paleomagnetic poles for Laurentia (not including separated terranes) compiled in this study for the Proterozoic and in Torsvik et al. (2012) for the Phanerozoic is shown.

and the Mesoproterozoic tectonic history is not as well elucidated as on the southern to eastern margin. The 15 to 20 km thick package of sedimentary rocks of the Belt-Purcell Supergroup is associated with a ca. 1.47 to 1.40 intracontinental rift – the tectonic setting of which is debated. Hoffman (1989) proposed that it may be a remanent back-arc basin trapped within a continent, while others envision it as being associated with continental rifting along the margin associated with separation of a conjugate continent (Jones et al., 2015). This region is interpreted to have been subsequently deformed during a ca. 1.36 to 1.33 event known as the East Kootenay orogeny (McMechan and Price, 1982; Nesheim et al., 2012; McFarlane, 2015).

This late Paleoproterozoic and Mesoproterozoic tectonic history provides significant constraints on paleogeographic reconstructions. In particular, the long-lived history of accretionary orogenesis along the southeast (present-day coordinates) of Laurentia from the initiation of the Yavapai orogeny (ca. 1.71 Ga) to the end of the Shawinigan orogeny (ca. 1.06 Ga) requires a long-lived open margin without a major conjugate continent until the time of terminal Grenvillian orogeny collision (Karlstrom et al., 2001). This constraint is incorporated into models such as that of Zhang et al. (2012) and Pehrsson et al. (2015) which maintain a long-lived convergent margin throughout the Mesoproterozoic, but in some reconstructions other continental blocks are reconstructed into positions that are seemingly incompatible with this record of accretionary orogenesis (e.g. Amazonia in Elming et al., 2009). The high-grade metamorphism associated with the Ottawan phase of the Grenvillian orogeny itself requires a collision between Laurentia and (an)other continent(s) ca. 1080 Ma – the geological observation of which first lead to the formulation of the hypothesis of the supercontinent Rodinia (Hoffman, 1991). Evidence of large-scale continent-continent collision at the time of the Ottawan Phase of the Grenvillian orogeny is recorded in Texas, up through the Blue Ridge Appalachian inliers, through Ontario and up to the Labrador Sea. This extensive and major collision orogenic history recorded in Laurentia remains a strong piece of evidence that a supercontinent or (proto)supercontinent formed at the 1.0 Ga Mesoproterozoic to Neoproterozoic transition. The term Grenville orogeny or Grenville belt is used rather loosely throughout much of the literature to refer to any late Mesoproterozoic orogenic belt. The timeline of orogenesis on the Laurentia margin has more nuanced constraints that this usage and these constraints can be comparatively assessed when

166 evaluating potential conjugate continents to Laurentia associated with the orogen (Fig. 2).

167 The subsequent Neoproterozoic tectonic history of Laurentia is dominantly a record of rifting
168 (Fig. 2). Along the western margin of Laurentia, small-scale rifting occurred ca. 780 to 720 Ma
169 leading to deposition in basins that is recorded from the Death Valley region of SW Laurentia up
170 to the Mackenzie Mountains of NW Laurentia (Macdonald et al., 2012; Rooney et al., 2017).
171 However, this extensional basin development is relatively minor and predates the more significant
172 rifting that lead to passive margin thermal subsidence that did not occur until the Ediacaran
173 Period (closer to the ca. 539 Ma Neoproterozoic-Phanerozoic boundary; Bond et al., 1984; Levy
174 and Christie-Blick, 1991). The emplacement of the ca. 780 Ma Gunbarrel large igneous province
175 along this margin and the subsequent extension recorded in the basins is commonly interpreted to
176 be associated with the break-up of Laurentia and a conjugate continent to the western margin. If
177 this interpretation is correct, it is unclear why there would be minimal thermal subsidence until
178 the Ediacaran (post 635 Ma as in Levy and Christie-Blick, 1991 and Witkosky and Wernicke,
179 2018). The geological evidence therefore supports active tectonism along the western margin of
180 Laurentia, but suggests that more dramatic lithospheric thinning occurred later than the timing
181 of rifting typically implemented in models of Rodinia break-up. One possibility, along the lines of
182 that proposed in Ross (1991), is that ca. 780 Ma extensional tectonism is an inboard record of
183 rifting and passive margin development that occurred further outboard. In this model,
184 subsequent continent rifting that drove lithospheric thinning, perhaps associated with the
185 departure of a microcontinent fragment rather than an already departed major conjugate
186 continent, would be the cause of Ediacaran to Cambrian thermal subsidence. The margin that
187 did experience large-scale rifting and associated passive margin thermal subsidence earlier in the
188 Neoproterozoic is the northeast Greenland margin (Fig. 2). Available geochronological
189 constraints and thermal subsidence modeling indicate ca. 820 Ma rifting followed by thermal
190 subsidence of a stable platform (Maloof et al., 2006; Halverson et al., 2018). These data suggest
191 that conjugate continental lithosphere rifted away from northeast Greenland ca. 820 Ma.

192 Extensive rifting that was followed by thermal subsidence occurred along the southeast to east
193 Laurentia margin leading up to the Neoproterozoic-Phanerozoic boundary and is interpreted to be
194 associated with the opening of the Iapetus ocean. A record of this rifting is preserved as rift

195 basins that were part of failed arms (Rome trough, Reelfoot rift and Oklahoma aulacogen; Fig. 1)
196 as well as prolonged Cambrian to Ordovician passive margin thermal subsidence along the margin
197 (Bond et al., 1984; Whitmeyer and Karlstrom, 2007). The age of igneous intrusions that have
198 been interpreted to be rift-related play a significant role in interpretations of this history such as
199 in the rift development model of Burton and Southworth (2010). In this model,
200 spatially-restricted rifting occurs ca. 760 to 680 Ma in the region of modern-day North Carolina
201 and Virginia. Rifting ca. 620 to 580 Ma initiates in the region from modern-day New York to
202 Newfoundland and by ca. 580 to 550 Ma rifting extends along the length of Laurentia's eastern
203 margin. The last phases of this rifting appears to be associated with the separation of the
204 Argentine pre-Cordillera Cuyania terrane (Dickerson and Keller, 1998). Cuyania is widely
205 interpreted be a rifted fragment of SE Laurentia that separated associated with this early
206 Cambrian rifting and subsequently became part of Gondwana when it collided with other terranes
207 in the vicinity of the Rio de Plata craton during the Ordovician Famatinian orogeny (Martin
208 et al., 2019). As with other rifts, it is difficult to distinguish the separation of a cratonic fragment
209 as a microcontinent from the rifting of a major craton as the record that lingers on the craton is
210 similar. One interpretation is that there was successful break-up along the eastern margin during
211 the ca. 580 to 550 Ma interval of rifting prior to the ca. 539 Oklahoma aulacogen rifting that
212 liberated the Cuyania microcontinent. The Maz–Arequipa–Rio Apa (MARA) block with which
213 Cuyania collided (Martin et al., 2019) is likely a product of such rifting. Orogenesis between the
214 MARA block and the Rio de Plata and Kalahari in the ca. 530 Ma Pampean orogeny (Casquet
215 et al., 2018) predated the collision of Cuyania during the ca. 460 Ma Famatinian orogeny in West
216 Gondwana (Rapalini, 2018).

217 The eastern margin of Laurentia then went through the cycle of Appalachian orogenesis. As is
218 visualized in Figure 2, there are parallels between the Grenville orogenic interval and the
219 Appalachian orogenic interval in that there was a period of arc-continent collision (Shawinigan
220 orogeny in the Grenville interval; Taconic orogeny in the Appalachian interval) followed by
221 microcontinent accretion (Llano in the Grenville interval; Acadian in the Appalachian interval)
222 that culminated in large-scale continent-continent collision (Grenvillian orogeny in the Grenville
223 interval; Alleghanian in the Appalachian interval). These similarities are the consequence of an

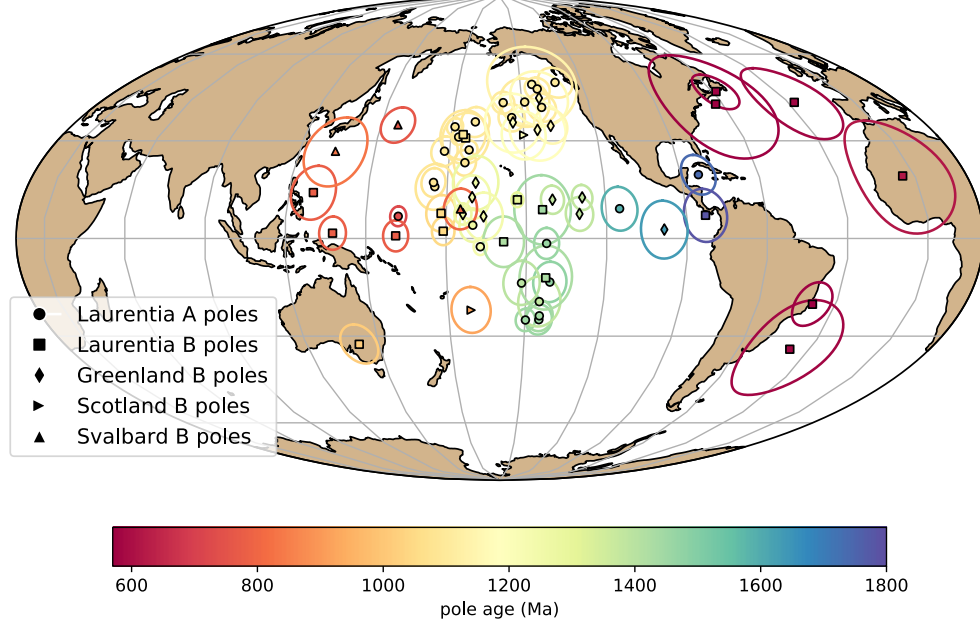
²²⁴ active margin facing an ocean basin that was progressively consumed until its consumption
²²⁵ resulted in continent-continent collision. In the case of the Grenville interval, this terminal
²²⁶ collision is interpreted to be associated with the assembly of the supercontinent Rodinia and in
²²⁷ the Appalachian interval it is interpreted to be associated with the assembly of the supercontinent
²²⁸ Pangea.

²²⁹ Even without considering other continents on Earth, the geological record of Paleoproterozoic
²³⁰ collisional of Archean provinces combined with accretionary orogenesis at that time and through
²³¹ the rest of the Paleoproterozoic and Mesoproterozoic Eras provides very strong evidence for
²³² mobile plate tectonics driving Laurentia's evolution throughout the past 2 billion years. This
²³³ tectonic history inferred from geological data can be enhanced through integration with the
²³⁴ paleomagnetic record.

²³⁵ 3.3 Paleomagnetic pole compilation

²³⁶ In this chapter, I focus on the compilation of paleomagnetic poles developed through the Nordic
²³⁷ Paleomagnetism Workshops with some additions and modifications (Fig. 3 and Table 2). The
²³⁸ Nordic Paleomagnetism Workshops have taken the approach of using expert panels to assess
²³⁹ paleomagnetic poles and assign them grades meant to convey the confidence that the community
²⁴⁰ has in these results (Evans et al., this volume). While many factors associated with
²⁴¹ paleomagnetic poles can be assessed quantitatively through Fisher statistics and the precision of
²⁴² geochronological constraints, other aspects such as the degree to which available field tests
²⁴³ constrain the magnetization to be primary require expert assessment. The categorizations used by
²⁴⁴ the expert panel are 'A' and 'B' with the last panel meeting occurring in Fall 2017 in Leirubakki,
²⁴⁵ Iceland. An 'A' rating refers to poles that are judged to be of such high-quality that they provide
²⁴⁶ essential constraints that should be satisfied in paleogeographic reconstructions. A 'B' rating is
²⁴⁷ associated with poles that are judged to likely provide a high-quality constraint, but have some
²⁴⁸ deficiency such as remaining ambiguity in the demonstration of primary remanence or the
²⁴⁹ quality/precision of available geochronologic constraints. Additional poles that were not given an
²⁵⁰ 'A' or 'B' classification at the Nordic Workshops are referred to as not-rated ('NR'). These
²⁵¹ additional poles are taken from the Paleomagia database (Veikkolainen et al., 2014). Many of

Poles for Laurentia (post-Paleoproterozoic amalgamation; with terranes)



Poles for Laurentia (pre-Paleoproterozoic amalgamation)

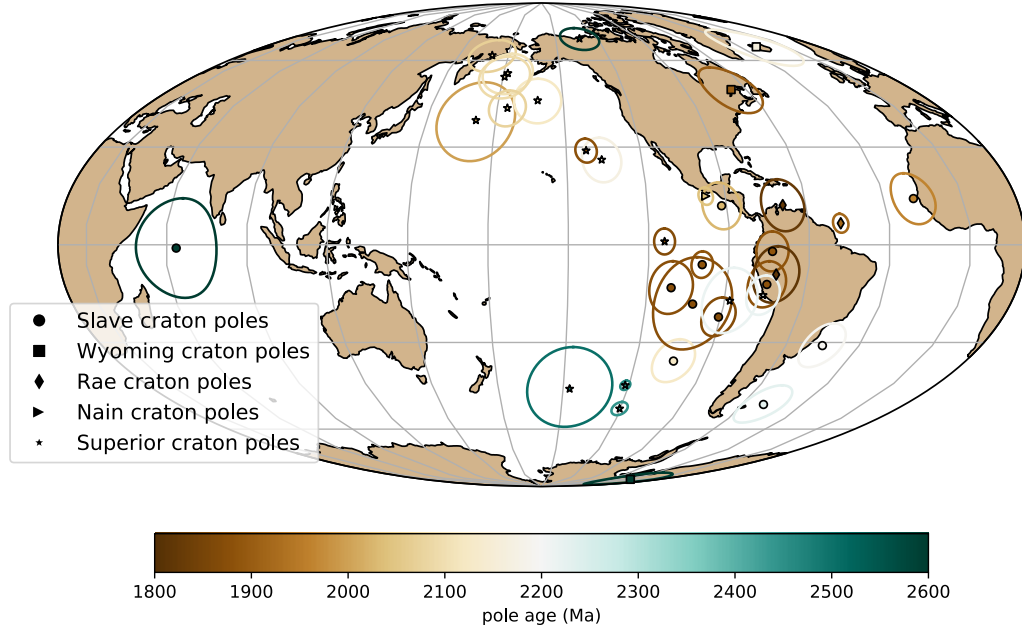


Figure 3. Top panel: Paleomagnetic poles from 1800 to 560 Ma for Laurentia (including Greenland, Scotland and Svalbard). Bottom panel: Paleomagnetic data for Archean Provinces prior to the amalgamation of Laurentia.

252 these poles are quite valuable for reconstruction and should not be dismissed from being
253 considered in paleogeographic reconstructions. However, there are ambiguities associated with
254 many of such poles not given Nordic ‘A’ or ‘B’ ratings in terms of how well the nature of the
255 remanence is constrained including its age. For example, there are rich data associated with
256 intrusive and metamorphic lithologies of the Grenville Province that are the available
257 paleomagnetic constraints for Laurentia at the Mesoproterozoic-Neoproterozoic boundary.
258 However, the ages of the remanence associated with these poles is complicated by the reality that
259 the magnetization was acquired during exhumation and such cooling ages are more difficult to
260 robustly constrain than the ages of remanence associated with dated eruptive units or
261 shallow-level intrusions. As a result, the vast majority of Grenville Province poles are not given
262 an ‘A’ or ‘B’ rating with the exception of the ‘B’ rated pole from the ca. 1015 Ma Haliburton
263 intrusions. However, while any one of these Grenville poles could be interpreted to suffer from
264 large temporal uncertainty, the overall preponderance of poles in a similar location at the time
265 suggests that they need to be taken seriously within any paleogeographic reconstruction of
266 Laurentia (although note an alternative view of an allochthonous origin put forward by Halls
267 et al. (2015) is discussed below). In this compilation, the poles of Brown and McEnroe (2012)
268 from the Adirondack highlands are used wherein the magnetic mineralogy and associated relative
269 ages of remanence are well-constrained (Table 2). Additional not-rated poles included in the
270 present compilation is the new pole for the ca. 1144 Ma Ontario lamprophyre dykes (Piispa et al.,
271 2018) that strengthens the position of Laurentia at the time and coincides with the position of the
272 poles from the ca. 1140 Ma Abitibi dikes (Ernst and Buchan, 1993). This pole will likely receive
273 an ‘A’ rating when assessed at the next Nordic paleomagnetism workshop. Poles from the
274 Neoproterozoic Chuar Group as presented in Eyster et al. (2019) are also included.

275 **3.4 Differential motion before Laurentia amalgamation**

276 Prior to the termination of the Trans-Hudson orogeny (before 1.8 Ga), paleomagnetic poles need
277 to be considered with respect to the individual Archean provinces. For the Superior province, an
278 additional complexity is that paleomagnetic poles from Siderian to Rhyacian Period (2.50 to 2.05
279 Ga) dike swarms, as well as deflection of dike trends, support an interpretation that there was

280 substantial Paleoproterozoic rotation of the western Superior province relative to the eastern
281 Superior province across the Kapuskasing Structural Zone (Bates and Halls, 1991; Evans and
282 Halls, 2010). This interpretation is consistent with the hypothesis of Hoffman (1988) that the
283 Kapuskasing Structural Zone represents major intracratonic uplift related to the Trans-Hudson
284 orogeny. Evans and Halls (2010) propose an Euler rotation of (51°N, 85°W, -14°CCW) to
285 reconstruct western Superior relative to eastern Superior and interpret that the rotation occurred
286 in the time interval of 2.07 to 1.87 Ga. I follow this interpretation and group the poles into
287 Superior (West) and Superior (East). Uncertainty remains with respect to whether the ca. 1.88
288 Ga Molson dikes pole pre-dates or post-dates this rotation (Evans and Halls, 2010) and thus for
289 the time being should be considered solely in the western Superior province reference frame.

290 There are poles in the compilation for the Slave, Wyoming, Rae, Superior and North Atlantic
291 provinces prior to Laurentia amalgamation (Fig. 3 and Table 2). Overall, these data provide an
292 opportunity to re-evaluate the paleomagnetic evidence for relative motions between Archean
293 provinces prior to Laurentia assembly. A lingering question raised in Hoffman (1988) that still
294 remains is to what extent the Archean provinces each had independent drift histories with
295 significant separation or shared histories before experiencing fragmentation and reamalgamation.
296 The strongest analysis in this regard comes from comparisons between paleomagnetic poles
297 between the Superior and Slave provinces (Buchan et al., 2009; Mitchell et al., 2014; Buchan
298 et al., 2016). High-quality paleomagnetic poles from these two provinces provide strong support
299 for differential motion between the Superior and Slave provinces between 2.2 and 1.8 Ga with the
300 two provinces not being in their modern-day relative orientation to one another either and having
301 distinct pole paths as constrained by 5 time periods of nearly coeval poles from 2.23 and 1.89 Ga
302 (Fig. 4; Buchan et al., 2016. These data provide paleomagnetic support for the Superior and
303 Slave provinces having independent histories of differential motion. They also support the
304 hypothesis that the Trans-Hudson orogeny is the result of terminal collision associated with the
305 closure of an ocean basin between the Superior province and the Hearne+Rae+Slave provinces.
306 Reconstructions developed for this chapter of the Superior and Slave provinces using these poles
307 are shown in Figure 4 and illustrate the difference in implied orientation and paleolatitude that
308 results from these well-constrained poles.

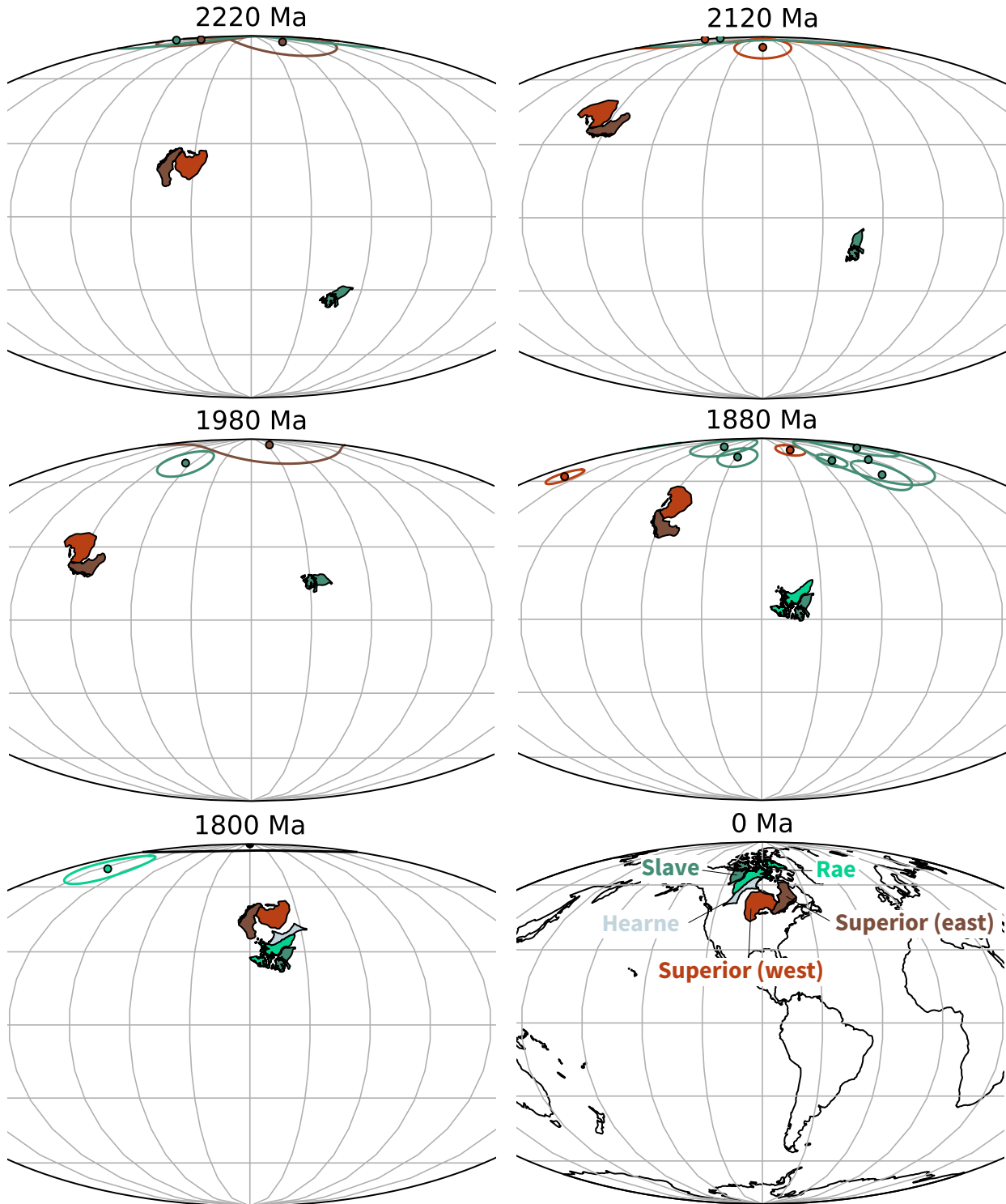


Figure 4. Paleogeographic reconstructions developed using poles from the Superior, Slave and Rae provinces. Paleomagnetic poles are shown colored to match their respective province with these provinces shown in present-day coordinates and labeled in the 0 Ma panel. Poles with ages that are within 25 million years of the given time slice are shown. The relatively well-resolved pole paths from the Superior and Slave provinces (Fig. 3) that are utilized for these reconstructions provide strong support for differential plate tectonic motion between 2220 and 1850 Ma.

³⁰⁹ **3.5 Paleogeography of an assembled Laurentia**

³¹⁰ Following the amalgamation of the Archean provinces in Laurentia ca. 1.8 Ga, poles from each
³¹¹ part of Laurentia can be considered to reflect the position of the entire composite craton. It is
³¹² worth considering the possibility that poles from zones of Paleoproterozoic and Mesoproterozoic
³¹³ accretion could be allochthonous to the craton. Halls (2015) argued that this was the case for late
³¹⁴ Mesoproterozoic and early Neoproterozoic poles from east of the Grenvillian allochthon boundary
³¹⁵ fault. However, the majority of researchers have considered these poles to post-date major
³¹⁶ differential motion and be associated with cooling during collapse of a thick orogenic plateau
³¹⁷ developed during continent-continent collision (e.g. Brown and McEnroe, 2012). Poles with a
³¹⁸ B-rating are also included in the composite that come from Greenland, Svalbard and Scotland.
³¹⁹ These terranes were once part of contiguous Laurentia, but have subsequently rifted away. These
³²⁰ poles need to be rotated into the Laurentia reference frame prior to use for tectonic
³²¹ reconstruction and I apply the rotations shown in Table 1. The Euler pole and rotation is quite
³²² well-constrained for Greenland as it is associated with recent opening of Baffin Bay and the
³²³ Labrador Sea (for which the rotation of Roest and Srivastava, 1989 is used). The reconstruction
³²⁴ of Scotland is associated with the opening of the Atlantic (for which the rotation employed by
³²⁵ Torsvik and Cocks, 2017 is used) which is well-constrained but has more uncertainty associated
³²⁶ with the Euler pole than that for Greenland. The reconstruction of Svalbard is more challenging
³²⁷ given a multi-state tectonic history involving both translation within the Caledonides and
³²⁸ subsequent rifting. The preferred Euler of Maloof et al. (2006) is used here. This Euler is
³²⁹ designed, in particular, to honor the high degree of similarity between Tonian sediments in East
³³⁰ Greenland (Hoffman et al., 2012) and those of East Svalbard (Maloof et al., 2006) and to
³³¹ reconstruct East Svalbard to be aligned with these correlative sedimentary rocks.

³³² Through the Proterozoic, there are intervals where there are abundant paleomagnetic poles
³³³ that constrain Laurentia's position and intervals when the record is quite sparse (shown colored
³³⁴ by age in Fig. 3). To further visualize the temporal coverage of the poles and to summarize the
³³⁵ motion, implied paleolatitudes for an interior point on Laurentia are shown in Figure 5. The ages
³³⁶ of the utilized paleomagnetic poles are also shown in comparison to the simplified summary of
³³⁷ tectonic events in Figure 2. Both collisional and extensional tectonism can result in the formation

338 of lithologies that can be used to develop paleomagnetic poles either as a result of basin
339 formation, magmatism or both. In addition, intraplate magmatism resulting from plume-related
340 large-igneous provinces can lead to paleomagnetic poles in periods that are otherwise
341 characterized by tectonic quiescence (e.g. the ca. 1267 Ma Mackenzie LIP; Fig. 2).

342 Intracontinental rifts have led to the highest density of poles both in the case of the ca. 1.4 Ga
343 Belt Supergroup and the ca. 1.1 Ga Midcontinent Rift (Fig. 2). The quality and resolution of the
344 record from the Midcontinent Rift is aided by the voluminous magmatism that occurred in
345 conjunction with basin formation that enables the development of well-calibrated apparent polar
346 wander path (Swanson-Hysell et al., 2019). The late Tonian Period also has a number of poles
347 including the Gunbarrel LIP (ca. 780 Ma) and Franklin LIP (ca. 720 Ma), as well as
348 similarly-aged sedimentary rocks from western Laurentia basins (Eyster et al., 2019). Overall,
349 there is internal consistency among the paleomagnetic poles within intervals for which there is
350 high-resolution coverage. These data result in progressive paths such as ascending up to the
351 Logan Loop, down the Keweenawan Track (Swanson-Hysell et al., 2019) to the Grenville Loop
352 prior to a temporal gap before the late Tonian (ca. 775 to 720 Ma) path (Eyster et al., 2019).

353 Data from other terranes add resolution to the record. In particular, data from Greenland
354 adds 12 poles between 1385 and 1160 Ma when there are only 4 poles from mainland Laurentia.
355 Given that the rotation between Greenland and mainland Laurentia is well-constrained (Table 1),
356 once rotated these poles can be used for reconstruction of the entire continent. The reliability of
357 this approach gains credence through the good agreement between the ca. 1633 Ma Melville Bugt
358 diabase dykes pole from Greenland (Halls et al., 2011) and the ca. 1590 Ma Western Channel
359 diabase pole of mainland Laurentia (Irving and Park, 1972). Similarly, there is good agreement
360 between the ca. 1267 Ma Mackenzie dykes pole of Laurentia (Buchan et al., 2000) and coeval
361 poles from Greenland such as the ca. 1275 Ma North Qoroq intrusives (Piper, 1992) and Kungnat
362 Ring dyke (Piper, 1977). Furthermore, the Greenland poles with ages that fall between the ca.
363 1237 Ma Sudbury dikes and ca. 1143 Ma lamprophyre dykes pole of mainland Laurentia are
364 consistent with constraints on either side from the mainland while filling in the ascending limb of
365 the path leading up to the apex of 1140 to 1108 Ma poles known as the Logan Loop (Fig. ??).

366 An exception to this overall agreement between poles from Greenland and mainland Laurentia

367 occurs ca. 1382 Ma. There are poles of this age from Greenland associated with the Zig-Zag Dal
368 basalts and related intrusions (Marcussen and Abrahamsen, 1983; Abrahamsen and Van Der Voo,
369 1987). However, these poles are in a distinct location from poles of similar age associated with the
370 Belt Supergroup (e.g. the McNamara Formation and Pilcher/Garnet Range and Libby
371 Formations; Elston et al., 2002). Additionally, the older Belt Supergroup poles form a more
372 southerly population than time-equivalent poles from elsewhere in Laurentia such as the Mistastin
373 Pluton. There are potential complications associated with the Belt Supergroup being exposed
374 within thrust sheets with significant Cenozoic Mesozoic and Cenozoic deformation. However,
375 vertical axis rotations of the Belt region are not able to bring the Belt poles into agreement with
376 those from Laurentia or Greenland nor is translation away from the craton. Another potential
377 complication is that the remanence used for the development of the Belt Supergroup resides in
378 hematite. As a result, there is the potential for inclination-flattening within the sedimentary rocks
379 from which poles are developed. However, applying a moderate inclination factor of $f = 0.6$ also
380 does not bring the poles into congruence with the Zig-Zag basalts. There is the potential that the
381 hematite could be the result of post-depositional oxidation (the remanence of the Purcell lavas
382 pole is also held by hematite) however the overall coherency of the pole directions and the
383 presence of reversals has been taken as evidence that the remanence is primary (Elston et al.,
384 2002). At present, it is unclear which poles are a better representation of Laurentia's position ca.
385 1400 Ma.

386 Another challenging portion of the Laurentia record is that for the Ediacaran Period where
387 there is little consistency between poles of similar age (Figs. 3 and ??). As a result, there are
388 poles that imply both low-latitude and high-latitude positions of Laurentia between 615 and 565
389 Ma. One explanation for these variable pole positions is that they are the result of large-scale
390 oscillatory true polar wander in the Ediacaran that has influenced poles in Baltica and West
391 Africa as well (McCausland et al., 2007; Robert et al., 2017). Another possibility is that the lack
392 of congruency between poles in this point in the record is due to a particularly weak and
393 non-dipolar geomagnetic field (Abrajevitch and Van der Voo, 2010; Bono et al., 2019). Regardless
394 of mechanism, the Ediacaran data stand out as anomalous relative to the coherency of the rest of
395 the poles in the composite (Fig. 5).

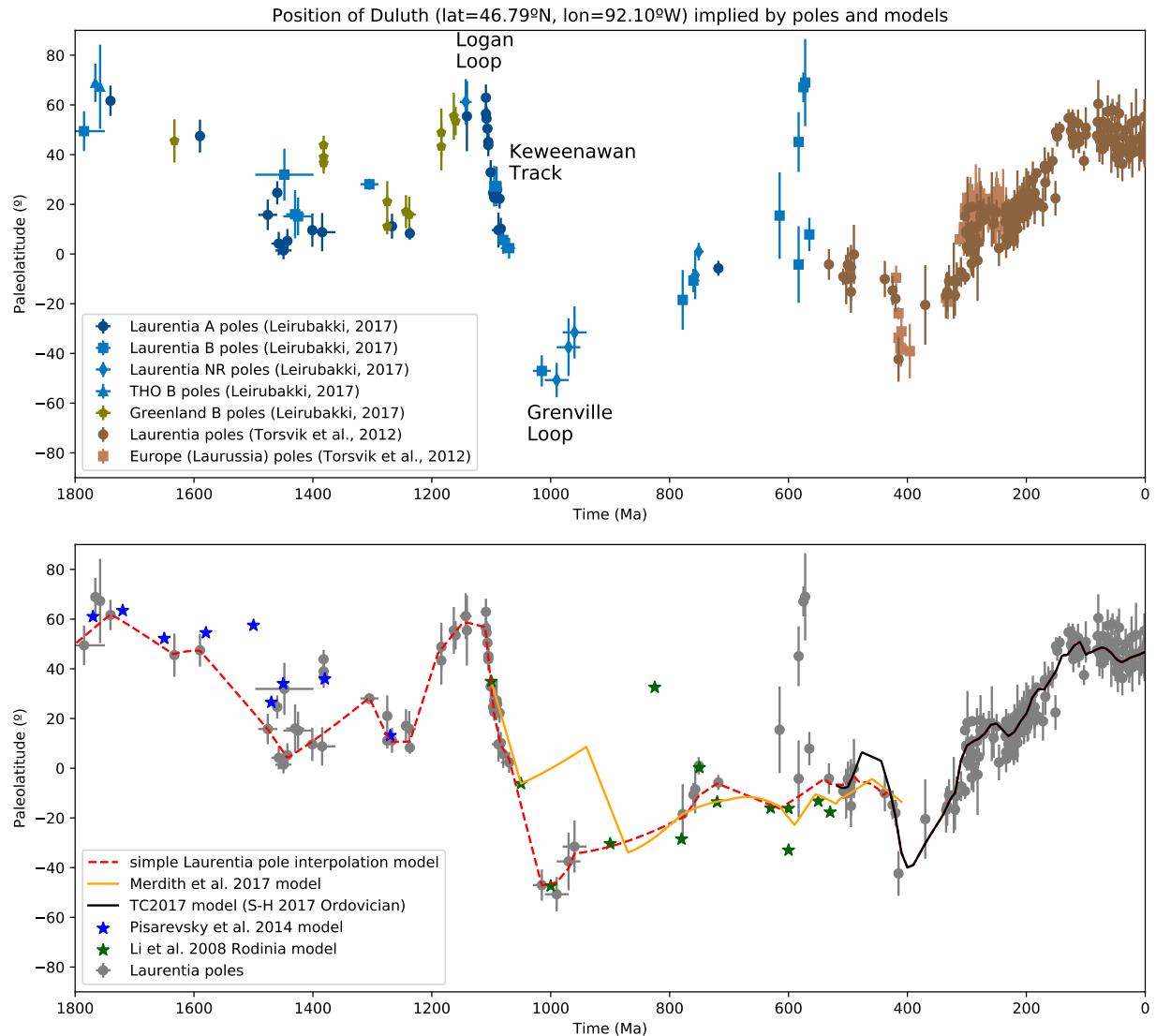


Figure 5. Top panel: Paleolatitude implied by paleomagnetic poles from Laurentia and associated blocks for Duluth (lat=46.79°N, lon=92.10°W). The paleomagnetic poles are compiled in Table 2. Bottom panel: Paleolatitude implied by Laurentia poles compared with that implied by published paleogeographic models and the simple Laurentia model used in this chapter for the reconstructions in Figure 6.

396 Synthesizing the compilation of paleomagnetic poles for Laurentia into a composite path over
397 the past 1.8 billion years presents a challenge given the highly variable temporal coverage. The
398 method typically applied in the Phanerozoic is to develop synthesized pole paths either through
399 fitting spherical splines through the data or calculating binned running means where the Fisher
400 mean of poles within a given interval are calculated (Torsvik et al., 2012). Applying such an
401 approach can reduce the effect of spurious poles in regions of high data density where seeking to
402 satisfy every mean pole position would result in jerky motion.

403 A synthesized pole path for Laurentia is developed here and used to develop a continuous
404 paleogeographic reconstruction of Laurentia constrained by the compilation of paleomagnetic
405 poles. The paleolatitude implied by this continuous model is shown in Figure 5. This path is
406 based on Laurentia data alone which means that it is poorly constrained through intervals of
407 sparse data (950-850 Ma for example). One could use interpretations of paleogeographic
408 connections with other cratons (e.g. Baltica in the early Neoproterozoic) to fill in such portions of
409 the path, however the result then becomes model-dependent without being constrained by data
410 from Laurentia itself. In portions of the record with a more dense record of poles, such as ca.
411 1450, a calculated running mean is used to integrate constraints from multiple poles. This
412 method follows the approach taken in the Phanerozoic (e.g. Torsvik et al., 2012 wherein all poles
413 within a 20 Myr interval are averaged with the interval than progressively moved forward in 10
414 Myr steps. When there are isolated ‘A’ grade poles without other temporally-similar poles, these
415 poles are fully satisfied in model. Where there are no constraints a simple interpolation between
416 constraints is made. While data from Scotland and Svalbard are associated with Laurentia, the
417 Scotland poles are poorly constrained in time and the Svalbard rotation to Laurentia is uncertain.
418 These poles are not utilized in the simple Laurentia model which means that the model as shown
419 does not include oscillatory true polar wander interpreted to have occurred ca. 810 and 790 Ma
420 based on data from Svalbard (Maloof et al., 2006).

421 One downside of a running mean approach is that it pulls the mean to regions of high data
422 density. As was shown in Swanson-Hysell et al. (2019), this behavior can reduce motion along an
423 apparent polar wander path. As a result, for the portion of the reconstruction during the interval
424 of time ca. 1110 to 1070 Ma, I utilize an Euler pole inversion from Swanson-Hysell et al. (2019).

425 Paleogeographic snapshots for the past position of Laurentia reconstructed using this synthesis
426 of the paleomagnetic poles are shown in Figure 6. These reconstructions use the tectonic elements
427 as defined by Whitmeyer and Karlstrom (2007) with these elements being progressively added
428 associated with Laurentia's accretionary growth. As a reminder to the reader, paleomagnetic
429 poles provide constraints on the paleolatitude of a continental block as well as its orientation
430 (which way was north relative to the block). While they provide constraints in this regard, they
431 do not provide constraints in and of themselves of the longitudinal position of the block. Other
432 approaches to obtain paleolongitude utilize geophysical hypotheses such as assuming that large
433 low shear velocity provinces have been stable plume-generating zones in the lower mantle to
434 which plumes can be reconstructed (Torsvik et al., 2014) or that significant pole motion in certain
435 time intervals is associated with true polar wander axes that switch through time in conjunction
436 with the supercontinent cycle (Mitchell et al., 2012). In Figure 6, Laurentia is centered on the
437 longitudinal position of Duluth with the orientation and paleolatitude being constrained by the
438 paleomagnetic pole compilation as synthesized in the simple Laurentia pole interpolation model.
439 The continuous paleolatitude implied by this model is shown as the simple Laurentia pole
440 interpolation mode in Figure 5.

441 3.6 Comparing paleogeographic models to the paleomagnetic compilation

442 Developing comprehensive global continuous paleogeographic models is a major challenge given
443 the need to integrate and satisfy diverse geological and paleomagnetic data types. Continually
444 improving constraints related to tectonic setting from improved geologic and geochronologic data
445 need to be carefully integrated with the database of paleomagnetic poles. Paleomagnetic poles
446 compilations themselves are evolving with better data and improved geochronology. Efforts such
447 as this volume are therefore essential to present the state-of-the-art in terms of existing
448 constraints that can be used to evaluate current models and set the stage for future progress in
449 Precambrian paleogeography.

450 There is an overall lack of models in the literature for the Proterozoic have published
451 continuous rotation parameters that can be compared to the compilation of paleomagnetic poles
452 presented herein. The approach in the community for many years has been to publish models as

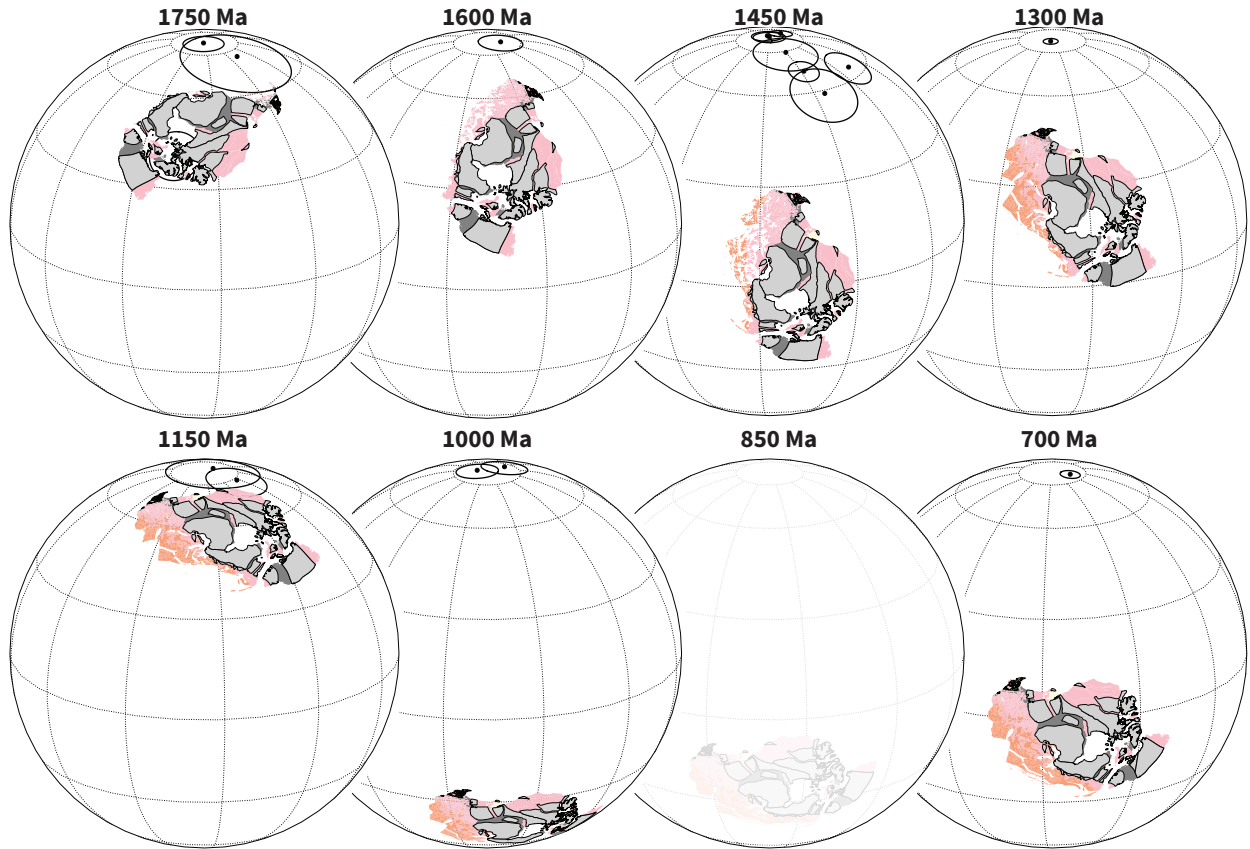


Figure 6. Paleogeographic reconstructions of Laurentia at time intervals through the Proterozoic that are well-constrained by paleomagnetic data. These reconstructions use the simple Laurentia pole interpolation model that is shown in Figure 5 and use this model to reconstruct the tectonic elements of Whitmeyer and Karlstrom (2007) shown in Figure 1. Modern coastlines are maintained in these polygons so that the rotated orientations can be interpreted by the reader in comparison to Figure 1. Paleomagnetic poles within 25 million years of each reconstruction time are plotted. All reconstructions have poles within such a time frame that provide constraints with the exception of the 850 Ma reconstruction which is shown faintly given this relative uncertainty in Laurentia's position.

453 snapshots at given time intervals presented in figures without publishing continuous rotation
454 parameters although some studies have published the Euler rotations associated with specified
455 times. With the further adoption of software tools such as GPlates, there has been significant
456 progress in the publication of continuous paleogeographic models constrained by paleomagnetic
457 poles through the Phanerozoic (540 Ma to present; e.g. Torsvik et al., 2012).

458 An exception to the paucity of published continuous paleogeographic models for the
459 Precambrian is the Neoproterozoic model of Merdith et al. (2017) which is shown in comparison
460 to the constraints for Laurentia in Figure 5. The extent to which the implied position of
461 Laurentia in Merdith et al. (2017) is consistent with the compiled paleomagnetic constraints can
462 be visualized in Figure 5. As noted above, the development of such models is challenging and the
463 researchers need to balance varying constraints. The focus here will be on the extent to which
464 this model satisfies the available paleomagnetic poles for Laurentia. The model does not honor
465 the Grenville loop (e.g. go to moderately high southerly latitudes ca. 1000 Ma) which is a striking
466 departure from the paleomagnetic record and standard paleogeographic models. Additionally, the
467 implemented plate motion strays from the younger poles of the Keweenawan Track and does not
468 honor the Franklin LIP pole Denyszyn et al. (2009b) despite its ‘A’ Nordic rating. The Franklin
469 pole is taken to be a key constraint at the Tonian/Cryogenian boundary that provides evidence of
470 the supercontinent Rodinia being equatorial and for the Sturtian glaciation having extended to
471 equatorial latitudes (Macdonald et al., 2010).

472 There are more published models that show snapshots and publish rotation parameters
473 associated with given time intervals such as the Rodinia model of Li et al. (2008) and the
474 Mesoproterozoic model of Pisarevsky et al. (2014), but did not publish parameters for a
475 continuous model. The position for Laurentia implied by the Euler poles given for the model
476 snapshots of these studies are shown in Figure 5 and can be compared to the compiled record.

477 3.7 Conclusion

478 There is strong evidence both in Laurentia’s geological and paleomagnetic record for differential
479 plate tectonic motion between 2.2 and 1.8 Ga. The continued history of accretionary orogenesis

and the evaluation of Laurentia's pole path in comparison to other continents from 1.8 Ga onward supports the continual operation of plate tectonics throughout the rest of the Proterozoic and Phanerozoic as well. While this evidence fits with the majority of interpretations of the timing of initiation of modern-style plate tectonics (see summary in Korenaga, 2013), there continue to be arguments proposing that a stagnant lid persisted through the Mesoproterozoic Era (1.6 to 1.0 Ga) and into the Neoproterozoic with plate tectonics not initiating until ca. 0.8 Ga (Hamilton, 2011; Stern and Miller, 2018). These arguments rest largely on the relative lack of Proterozoic low-temperature high-pressure metamorphic rocks such as blueschists that form in subduction zones (Stern et al., 2013). An alternative interpretation for this lack of blueschists in the Proterozoic is that such a shift in metamorphic regime is the predicted result of secular evolution of mantle chemistry rather than a harbinger of the onset of plate tectonics (Palin and White, 2015). While this line of evidence is intriguing, to argue that there was not differential plate tectonic motion in the Paleoproterozoic and Mesoproterozoic is to ignore a vast breadth and depth of geological and paleomagnetic data. From a paleomagnetic perspective, there is strong support for independent and differential motion of the Slave and Superior provinces as is illustrated in Figure 4. From a geological perspective, the Trans-Hudson orogenic cycle, the Grenville orogenic cycle, and the Appalachian orogenic cycle are all well-explained with a mobilistic interpretation that includes phases of accretionary followed by collisional orogenesis (Fig. 2). One could counter that this perspective results from a plate-tectonic-centric viewpoint that lacks creativity to see the record as resulting from other processes than modern-style plate tectonics. However, in addition to the broad geological record showing an amalgamation of terranes as would be expected to arise through plate tectonics, there are also eclogites preserved in the Trans-Hudson orogen that preserve evidence for high-pressure/low-temperature metamorphic conditions ca. 1.8 Ga (Weller and St-Onge, 2017). Similar to the Himalayan orogen, these rocks are interpreted to be the result of deep continental subduction and exhumation associated with convergent plate tectonics (Weller and St-Onge, 2017). Outside of Laurentia, there are examples of eclogites with geochemical affinity to oceanic crust such as that documented in the ca. 1.9 Ga Ubendian Belt of the Congo craton (Boniface et al., 2012).

Another perspective on Proterozoic tectonics, is that the record is one of intermittent

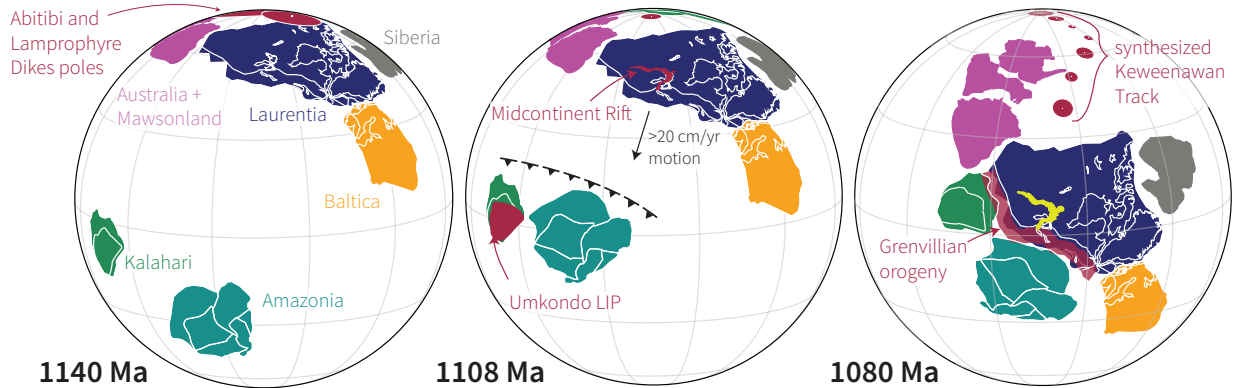


Figure 7. Paleogeographic reconstructions of Laurentia and other select Proterozoic continents leading up to Rodinia assembly in the late Mesoproterozoic modified from Swanson-Hysell et al. (2019). The record of paleomagnetic poles implies rapid motion which is consistent with the timing of collisional orogenesis associated with the Grenvillian orogeny.

509 subduction (Silver and Behn, 2008; O'Neill et al., 2013). In such a model, there are extended
 510 intervals with a stagnant lid alternating with intervals of differential plate motion. In particular,
 511 it was been argued that the Mesoproterozoic Era (1.6 to 1.0 Ga) is an interval when Earth was in
 512 a stagnant regime (Silver and Behn, 2008; O'Neill et al., 2013). The accretionary history of
 513 Laurentia following the amalgamation of the Archean provinces is difficult to reconcile with such
 514 an interpretation (Figs. 1 and 2). An additional constraint comes from the presence of reliable
 515 paleomagnetic poles themselves that are complete with baked contact tests. In a stagnant lid
 516 regime, there would not be sufficient heat flow to sustain a geodynamo and Earth should not have
 517 had a geomagnetic field that would have enable the preservation of paleomagnetic poles with
 518 positive field tests. The record of these poles also show that there was motion of Laurentia (Figs.
 519 5 and 6). Using data from Laurentia alone, however, it is difficult to ascertain whether this
 520 motion is due to plate tectonic motion or rotation of the entire solid Earth through true polar
 521 wander. True polar wander can lead to changing position relative to the spin axis even with a
 522 stagnant lid. One interval when the Laurentian paleomagnetic record demands that some of the
 523 motion is through differential plate tectonics is in the latest Mesoproterozoic. At that time, the
 524 pole path is very well-resolved with many high-quality paleomagnetic poles between 1110 and
 525 1070 Ma (Table 2; 3). The progression of the poles requires rotation about an Euler pole that is
 526 distinct from a great circle path which would result if the motion were solely due to true polar
 527 wander (Swanson-Hysell et al., 2019). These poles constrain rapid motion of Laurentia leading up
 528 to collisional orogenesis associated with the Grenvillian orogeny as illustrated in Figure 7. These

529 data provide strong evidence for differential plate motion at the time and are inconsistent with a
530 stagnant lid. Rather the orogenic cycle of the Mesoproterozoic bears similarity with that of the
531 Paleozoic and reveals Laurentia to have been a central player in the building of amalgamated
532 continents associated with Rodinia and Pangea.

533 The paleogeographic record of Laurentia is rich in constraints through the Precambrian both
534 in terms of the geological and geochronological constraints on tectonism and the record of
535 paleomagnetic poles. As can be seen in the Chapters on Archean paleogeography (Salminen et al.,
536 this volume), Nuna (Elming et al., this volume) and Rodinia (Evans et al., this volume), these
537 constraints are at the center of developing paleogeographic models through the Precambrian and
538 will continue to be moving forward.

539 Acknowledgements

540 Many participants in the Nordic Paleomagnetism Workshop have contributed to the compilation
541 and evaluation of the pole list utilized herein. Particular acknowledgement goes to David Evans
542 for maintaining and distributing the compiled pole lists as well as additional efforts of Lauri
543 Pesonen in maintaining the Paleomagia database (Veikkolainen et al., 2014). GPlates, and in
544 particular the pyGPlates API, was utilized in this work (Müller et al., 2018). Figures were made
545 using Matplotlib (Hunter, 2007) in conjunction with cartopy (Met Office, 2010 - 2015) and
546 pmagpy (Tauxe et al., 2016) within an interactive Python environment (Pérez and Granger,
547 2007). This work was supported by NSF CAREER Grant EAR-1847277 awarded to N.L.S.-H.
548 The code, data, and reconstructions used in this paper are openly available in this repository:
549 https://github.com/Swanson-Hysell-Group/Laurentia_Paleogeography.

550 References

- 551 Abrahamsen, N. and Van Der Voo, R., 1987, Palaeomagnetism of middle Proterozoic (c. 1.25 Ga) dykes from central
552 North Greenland: Geophysical Journal International, v. 91, p. 597–611, doi:10.1111/j.1365-246x.1987.tb01660.x.
- 553 Abrajevitch, A. and Van der Voo, R., 2010, Incompatible Ediacaran paleomagnetic directions suggest an equatorial
554 geomagnetic dipole hypothesis: Earth and Planetary Science Letters, v. 293, p. 164–170.

- 555 Bates, M. P. and Halls, H. C., 1991, Broad-scale Proterozoic deformation of the central Superior Province revealed
556 by paleomagnetism of the 2.45 Ga Matachewan dyke swarm: Canadian Journal of Earth Sciences, v. 28, p.
557 1780–1796, doi:10.1139/e91-159.
- 558 Berman, R., Davis, A., and Pehrsson, S., 2007, Collisional Snowbird tectonic zone resurrected: Growth of Laurentia
559 during the 1.9 Ga accretionary phase of the Hudsonian orogeny: Geology, v. 35, p. 911–914,
560 doi:10.1130/G23771A.1.
- 561 Bickford, M., Van Schmus, W., Karlstrom, K., Mueller, P., and Kamenov, G., 2015,
562 Mesoproterozoic-trans-Laurentian magmatism: A synthesis of continent-wide age distributions, new SIMS U–Pb
563 ages, zircon saturation temperatures, and Hf and Nd isotopic compositions: Precambrian Research, v. 265, p.
564 286–312, doi:10.1016/j.precamres.2014.11.024.
- 565 Bond, G., Nickleson, P., and Kominz, M., 1984, Breakup of a supercontinent between 625 and 555 Ma: new
566 evidence and implications for continental histories: Earth and Planetary Science Letters, v. 70, p. 325–345,
567 doi:10.1016/0012-821X(84)90017-7.
- 568 Boniface, N., Schenk, V., and Appel, P., 2012, Paleoproterozoic eclogites of MORB-type chemistry and three
569 Proterozoic orogenic cycles in the Ubendian Belt (Tanzania): Evidence from monazite and zircon geochronology,
570 and geochemistry: Precambrian Research, v. 192–195, p. 16–33, doi:10.1016/j.precamres.2011.10.007.
- 571 Bono, R. K., Tarduno, J. A., Nimmo, F., and Cottrell, R. D., 2019, Young inner core inferred from Ediacaran
572 ultra-low geomagnetic field intensity: Nature Geoscience, v. 12, p. 143–147, doi:10.1038/s41561-018-0288-0.
- 573 Books, K., 1972, Paleomagnetism of some Lake Superior Keweenawan rocks: U.S. Geological Survey Professional
574 Paper, v. P 0760, p. 42.
- 575 Borradaile, G. and Middleton, R., 2006, Proterozoic paleomagnetism in the Nipigon Embayment of northern
576 Ontario: Pillar Lake Lava, Wawieg Troctolite and Gunflint Formation tuffs: Precambrian Research, v. 144, p.
577 69–91, doi:10.1016/j.precamres.2005.10.007.
- 578 Brown, L. L. and McEnroe, S. A., 2012, Paleomagnetism and magnetic mineralogy of Grenville metamorphic and
579 igneous rocks, Adirondack Highlands, USA: Precambrian Research, v. 212–213, p. 57–74,
580 doi:10.1016/j.precamres.2012.04.012.
- 581 Buchan, K., Mertanen, S., Park, R., Pesonen, L., Elming, S. A., Abrahamsen, N., and Bylund, G., 2000, Comparing
582 the drift of Laurentia and Baltica in the Proterozoic: the importance of key paleomagnetic poles:
583 Tectonophysics, v. 319, p. 167–198.
- 584 Buchan, K. L., LeCheminant, A. N., and van Breemen, O., 2009, Paleomagnetism and U–Pb geochronology of the
585 Lac de Gras diabase dyke swarm, Slave Province, Canada: implications for relative drift of Slave and Superior
586 provinces in the Paleoproterozoic: Canadian Journal of Earth Sciences, v. 46, p. 361–379, doi:10.1139/e09-026.

- 587 Buchan, K. L., LeCheminant, A. N., and van Breemen, O., 2012, Malley diabase dykes of the Slave craton,
588 Canadian Shield: U–Pb age, paleomagnetism, and implications for continental reconstructions in the early
589 Paleoproterozoic: *Canadian Journal of Earth Sciences*, v. 49, p. 435–454, doi:10.1139/e11-061.
- 590 Buchan, K. L., Mitchell, R. N., Bleeker, W., Hamilton, M. A., and LeCheminant, A. N., 2016, Paleomagnetism of
591 ca. 2.13–2.11 Ga Indin and ca. 1.885 Ga Ghost dyke swarms of the Slave craton: Implications for the Slave
592 craton APW path and relative drift of Slave, Superior and Siberian cratons in the Paleoproterozoic: *Precambrian*
593 *Research*, v. 275, p. 151–175, doi:10.1016/j.precamres.2016.01.012.
- 594 Buchan, K. L., Mortensen, J. K., and Card, K. D., 1993, Northeast-trending early Proterozoic dykes of southern
595 Superior Province: multiple episodes of emplacement recognized from integrated paleomagnetism and U–Pb
596 geochronology: *Canadian Journal of Earth Sciences*, v. 30, p. 1286–1296, doi:10.1139/e93-110.
- 597 Burton, W. C. and Southworth, S., 2010, A model for Iapetan rifting of Laurentia based on Neoproterozoic dikes
598 and related rocks: From Rodinia to Pangea: The Lithotectonic Record of the Appalachian Region, p. 455–476,
599 doi:10.1130/2010.1206(20).
- 600 Casquet, C., Dahlquist, J. A., Verdecchia, S. O., Baldo, E. G., Galindo, C., Rapela, C. W., Pankhurst, R. J.,
601 Morales, M. M., Murra, J. A., and Mark Fanning, C., 2018, Review of the Cambrian Pampean orogeny of
602 Argentina; a displaced orogen formerly attached to the Saldania Belt of South Africa?: *Earth-Science Reviews*, v.
603 177, p. 209–225, doi:10.1016/j.earscirev.2017.11.013.
- 604 Condit, C. B., Mahan, K. H., Ault, A. K., and Flowers, R. M., 2015, Foreland-directed propagation of high-grade
605 tectonism in the deep roots of a Paleoproterozoic collisional orogen, SW Montana, USA: *Lithosphere*, p. L460.1,
606 doi:10.1130/l460.1.
- 607 Corrigan, D., Pehrsson, S., Wodicka, N., and de Kemp, E., 2009, The Palaeoproterozoic Trans-Hudson Orogen: a
608 prototype of modern accretionary processes: *Geological Society, London, Special Publications*, v. 327, p. 457–479,
609 doi:10.1144/sp327.19.
- 610 Dahl, P. S., Holm, D. K., Gardner, E. T., Hubacher, F. A., and Foland, K. A., 1999, New constraints on the timing
611 of Early Proterozoic tectonism in the Black Hills (South Dakota), with implications for docking of the Wyoming
612 province with Laurentia: *Geological Society of America Bulletin*, v. 111, p. 1335–1349,
613 doi:10.1130/0016-7606(1999)111<1335:ncotto>2.3.co;2.
- 614 Denyszyn, S. W., Davis, D. W., and Halls, H. C., 2009a, Paleomagnetism and U–Pb geochronology of the Clarence
615 Head dykes, Arctic Canada: orthogonal emplacement of mafic dykes in a large igneous province: *Canadian*
616 *Journal of Earth Sciences*, v. 46, p. 155–167, doi:10.1139/E09-011.
- 617 Denyszyn, S. W., Halls, H. C., Davis, D. W., and Evans, D. A. D., 2009b, Paleomagnetism and U–Pb geochronology
618 of Franklin dykes in High Arctic Canada and Greenland: a revised age and paleomagnetic pole constraining block
619 rotations in the Nares Strait region: *Canadian Journal of Earth Sciences*, v. 46, p. 689–705, doi:10.1139/E09-042.

- 620 Dickerson, P. W. and Keller, M., 1998, The Argentine Precordillera: its odyssey from the Laurentian Ouachita
621 margin towards the Sierras Pampeanas of Gondwana: Geological Society, London, Special Publications, v. 142,
622 p. 85–105, doi:10.1144/gsl.sp.1998.142.01.05.
- 623 Donadini, F., Pesonen, L. J., Korhonen, K., Deutsch, A., and Harlan, S. S., 2011, Paleomagnetism and
624 paleointensity of the 1.1 Ga old diabase sheets from central Arizona: Geophysica, v. 47, p. 3–30.
- 625 Elming, S. Å., D'Agrella-Filho, M. S., Page, L. M., Tohver, E., Trindade, R. I. F., Pacca, I. I. G., Geraldes, M. C.,
626 and Teixeira, W., 2009, A palaeomagnetic and 40Ar/39Ar study of late precambrian sills in the SW part of the
627 Amazonian craton: Amazonia in the Rodinia reconstruction: Geophysical Journal International, v. 178, p.
628 106–122.
- 629 Elston, D. P., Enkin, R. J., Baker, J., and Kisilevsky, D. K., 2002, Tightening the Belt: Paleomagnetic-stratigraphic
630 constraints on deposition, correlation, and deformation of the Middle Proterozoic (ca. 1.4 Ga) Belt-Purcell
631 Supergroup, United States and Canada: GSA Bulletin, v. 114, p. 619–638,
632 doi:10.1130/0016-7606(2002)114<619:TTBPSC>2.0.CO;2.
- 633 Emslie, R. F., Irving, E., and Park, J. K., 1976, Further paleomagnetic results from the Michikamau Intrusion,
634 Labrador: Canadian Journal of Earth Sciences, v. 13, p. 1052–1057, doi:10.1139/e76-108.
- 635 Ernst, R. and Buchan, K., 1993, Paleomagnetism of the Abitibi dike swarm, southern Superior Province, and
636 implications for the Logan Loop: Canadian Journal of Earth Science, v. 30, p. 1886–1897, doi:10.1139/e93-167.
- 637 Evans, D. and Halls, H., 2010, Restoring Proterozoic deformation within the Superior craton: Precambrian
638 Research, v. 183, p. 474 – 489, doi:10.1016/j.precamres.2010.02.007.
- 639 Evans, M. E. and Bingham, D. K., 1973, Paleomagnetism of the Precambrian Martin Formation, Saskatchewan:
640 Canadian Journal of Earth Sciences, v. 10, p. 1485–1493, doi:10.1139/e73-141.
- 641 Evans, M. E. and Hoye, G. S., 1981, Paleomagnetic results from the lower proterozoic rocks of Great Slave Lake and
642 Bathurst Inlet areas, Northwest Territories: *In* Proterozoic Basins of Canada; Geological Survey of Canada,
643 Paper 81-10, Natural Resources Canada/ESS/Scientific and Technical Publishing Services, doi:10.4095/109374.
- 644 Eyster, A., Weiss, B. P., Karlstrom, K., and Macdonald, F. A., 2019, Paleomagnetism of the Chuar Group and
645 evaluation of the late Tonian Laurentian apparent polar wander path with implications for the makeup and
646 breakup of Rodinia: GSA Bulletin, doi:10.1130/b32012.1.
- 647 Fahrig, W. and Bridgwater, D., 1976, Late Archean-early Proterozoic paleomagnetic pole positions from west
648 Greenland: *In* Windley, B., ed., Early History of the Earth, Wiley, p. 427–442.
- 649 Fahrig, W. F. and Jones, D. L., 1976, The paleomagnetism of the Helikian Mistastin pluton, Labrador, Canada:
650 Canadian Journal of Earth Sciences, v. 13, p. 832–837, doi:10.1139/e76-086.

- 651 Fairchild, L. M., Swanson-Hysell, N. L., Ramezani, J., Sprain, C. J., and Bowring, S. A., 2017, The end of
652 Midcontinent Rift magmatism and the paleogeography of Laurentia: *Lithosphere*, v. 9, p. 117–133,
653 doi:10.1130/L580.1.
- 654 Gala, M. G., Symons, D. T. A., and Palmer, H. C., 1995, Paleomagnetism of the Jan Lake Granite, Trans-Hudson
655 Orogen: *Saskatchewan Geological Survey Summary of Investigations*, v. 95-4.
- 656 Halls, H., 1974, A paleomagnetic reversal in the Osler Volcanic Group, northern Lake Superior: *Canadian Journal*
657 of *Earth Science*, v. 11, p. 1200–1207, doi:10.1139/e74-113.
- 658 Halls, H. C., 2015, Paleomagnetic evidence for ~4000 km of crustal shortening across the 1 Ga Grenville orogen of
659 North America: *Geology*, v. 43, p. 1051–1054, doi:10.1130/G37188.1.
- 660 Halls, H. C., Davis, D. W., Stott, G. M., Ernst, R. E., and Hamilton, M. A., 2008, The Paleoproterozoic Marathon
661 Large Igneous Province: New evidence for a 2.1 Ga long-lived mantle plume event along the southern margin of
662 the North American Superior Province: *Precambrian Research*, v. 162, p. 327–353,
663 doi:10.1016/j.precamres.2007.10.009.
- 664 Halls, H. C., Hamilton, M. A., and Denyszyn, S. W., 2011, The Melville Bugt Dyke Swarm of Greenland: A
665 Connection to the 1.5–1.6 Ga Fennoscandian Rapakivi Granite Province?, Springer Berlin Heidelberg, p. 509–535:
666 doi:10.1007/978-3-642-12496-9{_}27.
- 667 Halls, H. C. and Hanes, J. A., 1999, Paleomagnetism, anisotropy of magnetic susceptibility, and argon–argon
668 geochronology of the Clearwater anorthosite, Saskatchewan, Canada: *Tectonophysics*, v. 312, p. 235–248,
669 doi:10.1016/s0040-1951(99)00166-3.
- 670 Halls, H. C., Lovette, A., Hamilton, M., and Söderlund, U., 2015, A paleomagnetic and u–pb geochronology study
671 of the western end of the grenville dyke swarm: Rapid changes in paleomagnetic field direction at ca.
672 585 ma related to polarity reversals?: *Precambrian Research*, v. 257, p. 137–166,
673 doi:<http://dx.doi.org/10.1016/j.precamres.2014.11.029>.
- 674 Halverson, G. P., Porter, S. M., and Gibson, T. M., 2018, Dating the late Proterozoic stratigraphic record:
675 Emerging Topics in Life Sciences, v. 2, p. 137–147, doi:10.1042/etls20170167.
- 676 Hamilton, W. B., 2011, Plate tectonics began in Neoproterozoic time, and plumes from deep mantle have never
677 operated: *Lithos*, v. 123, p. 1–20, doi:10.1016/j.lithos.2010.12.007.
- 678 Harlan, S., 1993, Paleomagnetism of Middle Proterozoic diabase sheets from central Arizona: *Canadian Journal of*
679 *Earth Science*, v. 30, p. 1415–1426.
- 680 Harlan, S., Geissman, J., and Snee, L., 1997, Paleomagnetic and $^{40}\text{Ar}/^{39}\text{Ar}$ geochronologic data from late
681 Proterozoic mafic dykes and sills, Montana and Wyoming: *USGS Professional Paper*, v. 1580, p. 16.

- 682 Harlan, S. S. and Geissman, J. W., 1998, Paleomagnetism of the middle Proterozoic Electra Lake Gabbro, Needle
683 Mountains, southwestern Colorado: *Journal of Geophysical Research: Solid Earth*, v. 103, p. 15,497–15,507,
684 doi:10.1029/98jb01350.
- 685 Harlan, S. S., Geissman, J. W., and Snee, L. W., 2008, Paleomagnetism of Proterozoic mafic dikes from the Tobacco
686 Root Mountains, southwest Montana: *Precambrian Research*, v. 163, p. 239–264.
- 687 Harlan, S. S., Snee, L. W., Geissman, J. W., and Brearley, A. J., 1994, Paleomagnetism of the middle proterozoic
688 laramie anorthosite complex and sherman granite, southern laramie range, wyoming and colorado: *Journal of
689 Geophysical Research: Solid Earth*, v. 99, p. 17,997–18,020, doi:10.1029/94jb00580.
- 690 Henry, S., Mauk, F., and Van der Voo, R., 1977, Paleomagnetism of the upper Keweenawan sediments: Nonesuch
691 Shale and Freda Sandstone: *Canadian Journal of Earth Science*, v. 14, p. 1128–1138, doi:10.1139/e77-103.
- 692 Hildebrand, R. S., Hoffman, P. F., and Bowring, S. A., 2009, The Calderian orogeny in Wopmay orogen (1.9 Ga),
693 northwestern Canadian Shield: *Geological Society of America Bulletin*, v. 122, p. 794–814, doi:10.1130/B26521.1.
- 694 Hnat, J. S., van der Pluijm, B. A., and Van der Voo, R., 2006, Primary curvature in the Mid-Continent Rift:
695 Paleomagnetism of the Portage Lake Volcanics (northern Michigan, USA): *Tectonophysics*, v. 425, p. 71–82,
696 doi:10.1016/j.tecto.2006.07.006.
- 697 Hoffman, P., 1991, Did the breakout of Laurentia turn Gondwana inside out?: *Science*, v. 252, p. 1409–1412.
- 698 Hoffman, P. F., 1988, United plates of America, the birth of a craton: Early Proterozoic assembly and growth of
699 Laurentia: *Annual Review of Earth and Planetary Sciences*, v. 16, p. 543–603,
700 doi:10.1146/annurev.ea.16.050188.002551.
- 701 Hoffman, P. F., 1989, Speculations on Laurentia's first gigayear (2.0 to 1.0 Ga): *Geology*, v. 17, p. 135–138,
702 doi:10.1130/0091-7613(1989)017<0135:SOLSGF>2.3.CO;2.
- 703 Hoffman, P. F., Halverson, G. P., Domack, E. W., Maloof, A. C., Swanson-Hysell, N. L., and Cox, G. M., 2012,
704 Cryogenian glaciations on the southern tropical paleomargin of Laurentia (NE Svalbard and East Greenland),
705 and a primary origin for the upper Russøya (Islay) carbon isotope excursion: *Precambrian Research*, v. 206–207,
706 p. 137–158, doi:10.1016/j.precamres.2012.02.018.
- 707 Holm, D. K., Van Schmus, W. R., MacNeill, L. C., Boerboom, T. J., Schweitzer, D., and Schneider, D., 2005, U-Pb
708 zircon geochronology of Paleoproterozoic plutons from the northern midcontinent, USA: Evidence for subduction
709 flip and continued convergence after geon 18 Penokean orogenesis: *Geological Society of America Bulletin*, v. 117,
710 p. 259, doi:10.1130/b25395.1.
- 711 Hrncir, J., Karlstrom, K., and Dahl, P., 2017, Wyoming on the run—Toward final Paleoproterozoic assembly of
712 Laurentia: COMMENT: *Geology*, v. 45, p. e411–e411, doi:10.1130/g38826c.1.

- 713 Hunter, J. D., 2007, Matplotlib: A 2D graphics environment: Computing in Science & Engineering, v. 9, p. 90–95,
714 doi:10.1109/MCSE.2007.55.
- 715 Irving, E., 2004, Early Proterozoic geomagnetic field in western Laurentia: implications for paleolatitudes, local
716 rotations and stratigraphy: Precambrian Research, v. 129, p. 251–270, doi:10.1016/j.precamres.2003.10.002.
- 717 Irving, E. and McGlynn, J. C., 1979, Palaeomagnetism in the Coronation Geosyncline and arrangement of
718 continents in the middle Proterozoic: Geophysical Journal International, v. 58, p. 309–336,
719 doi:10.1111/j.1365-246X.1979.tb01027.x.
- 720 Irving, E. and Park, J. K., 1972, Hairpins and superintervals: Canadian Journal of Earth Sciences, v. 9, p.
721 1318–1324, doi:10.1139/e72-115.
- 722 Jones, J. V., Daniel, C. G., and Doe, M. F., 2015, Tectonic and sedimentary linkages between the Belt-Purcell basin
723 and southwestern Laurentia during the Mesoproterozoic, ca. 1.60–1.40 Ga: Lithosphere, v. 7, p. 465–472,
724 doi:10.1130/l438.1.
- 725 Karlstrom, K. E., Ahall, K.-I., Harlan, S. S., Williams, M. L., McLelland, J., and Geissman, J. W., 2001, Long-lived
726 (1.8–1.0 Ga) convergent orogen in southern Laurentia, its extensions to Australia and Baltica, and implications
727 for refining Rodinia: Precambrian Research, v. 111, p. 5–30, doi:10.1016/S0301-9268(01)00154-1.
- 728 Karlstrom, K. E. and Bowring, S. A., 1988, Early Proterozoic assembly of tectonostratigraphic terranes in
729 southwestern North America: The Journal of Geology, v. 96, p. 561–576, doi:10.1086/629252.
- 730 Kean, W., Williams, I., and Feeney, J., 1997, Magnetism of the Keweenawan age Chengwatana lava flows, northwest
731 Wisconsin: Geophysical Research Letters, v. 24, p. 1523–1526, doi:10.1029/97gl00993.
- 732 Kilian, T. M., Bleeker, W., Chamberlain, K., Evans, D. A. D., and Cousens, B., 2015, Palaeomagnetism,
733 geochronology and geochemistry of the Palaeoproterozoic Rabbit Creek and Powder River dyke swarms:
734 implications for Wyoming in supercraton Superia: Geological Society, London, Special Publications, v. 424, p.
735 15–45, doi:10.1144/sp424.7.
- 736 Kilian, T. M., Chamberlain, K. R., Evans, D. A., Bleeker, W., and Cousens, B. L., 2016, Wyoming on the
737 run—Toward final Paleoproterozoic assembly of Laurentia: Geology, v. 44, p. 863–866, doi:10.1130/g38042.1.
- 738 Korenaga, J., 2013, Initiation and evolution of plate tectonics on earth: Theories and observations: Annual Review
739 of Earth and Planetary Sciences, v. 41, p. 117–151, doi:10.1146/annurev-earth-050212-124208.
- 740 Kulakov, E. V., Smirnov, A. V., and Diehl, J. F., 2013, Paleomagnetism of ~1.09 Ga Lake Shore Traps (Keweenaw
741 Peninsula, Michigan): new results and implications: Canadian Journal of Earth Sciences, v. 50, p. 1085–1096,
742 doi:10.1139/cjes-2013-0003.

- 743 Levy, M. and Christie-Blick, N., Nicholas, 1991, Tectonic subsidence of the early Paleozoic passive continental
744 margin in eastern California and southern Nevada: Geological Society of America Bulletin, v. 103, p. 1590–1606,
745 doi:10.1130/0016-7606(1991)103<1590:tsotep>2.3.co;2.
- 746 Li, Z. X. et al., 2008, Assembly, configuration, and break-up history of Rodinia: A synthesis: Precambrian
747 Research, v. 160, p. 179–210, doi:10.1016/j.precamres.2007.04.021.
- 748 Macdonald, F., Halverson, G., Strauss, J., Smith, E., Cox, G., Sperling, E., and Roots, C., 2012, Early
749 Neoproterozoic basin formation in Yukon, Canada: Implications for the make-up and break-up of Rodinia:
750 Geoscience Canada, v. 39.
- 751 Macdonald, F. A., Schmitz, M. D., Crowley, J. L., Roots, C. F., Jones, D. S., Maloof, A. C., Strauss, J. V., Cohen,
752 P. A., Johnston, D. T., and Schrag, D. P., 2010, Calibrating the Cryogenian: Science, v. 327, p. 1241–1243,
753 doi:10.1126/science.1183325.
- 754 Maloof, A., Halverson, G., Kirschvink, J., Schrag, D., Weiss, B., and Hoffman, P., 2006, Combined paleomagnetic,
755 isotopic and stratigraphic evidence for true polar wander from the Neoproterozoic Akademikerbreen Group,
756 Svalbard, Norway: Geological Society of America Bulletin, v. 118, p. 1099–1124, doi:10.1130/B25892.1.
- 757 Marcussen, C. and Abrahamsen, N., 1983, Palaeomagnetism of the Proterozoic Zig-Zag Dal Basalt and the
758 Midsommerso Dolerites, eastern North Greenland: Geophysical Journal International, v. 73, p. 367–387,
759 doi:10.1111/j.1365-246x.1983.tb03321.x.
- 760 Martin, E. L., Collins, W. J., and Spencer, C. J., 2019, Laurentian origin of the Cuyania suspect terrane, western
761 Argentina, confirmed by Hf isotopes in zircon: GSA Bulletin, doi:10.1130/b35150.1.
- 762 McCausland, P. J. A., Hankard, F., Van der Voo, R., and Hall, C. M., 2011, Ediacaran paleogeography of
763 Laurentia: Paleomagnetism and 40Ar-39Ar geochronology of the 583 Ma Baie des Moutons syenite, Quebec:
764 Precambrian Research, v. 187, p. 58–78, doi:10.1016/j.precamres.2011.02.004.
- 765 McCausland, P. J. A., Van der Voo, R., and Hall, C. M., 2007, Circum-Iapetus paleogeography of the
766 Precambrian–Cambrian transition with a new paleomagnetic constraint from Laurentia: Precambrian Research,
767 v. 156, p. 125–152, doi:10.1016/j.precamres.2007.03.004.
- 768 McFarlane, C. R., 2015, A geochronological framework for sedimentation and Mesoproterozoic tectono-magmatic
769 activity in lower Belt–Purcell rocks exposed west of Kimberley, British Columbia: Canadian Journal of Earth
770 Sciences, v. 52, p. 444–465, doi:10.1139/cjes-2014-0215.
- 771 McGlynn, J. C., Hanson, G. N., Irving, E., and Park, J. K., 1974, Paleomagnetism and age of Nonacho Group
772 sandstones and associated Sparrow dikes, District of Mackenzie: Canadian Journal of Earth Sciences, v. 11, p.
773 30–42, doi:10.1139/e74-003.

- 774 McLelland, J. M., Selleck, B. W., and Bickford, M., 2010, Review of the Proterozoic evolution of the Grenville
775 Province, its Adirondack outlier, and the Mesoproterozoic inliers of the Appalachians: From Rodinia to Pangea:
776 The Lithotectonic Record of the Appalachian Region, p. 21–49, doi:10.1130/2010.1206(02).
- 777 McLelland, J. M., Selleck, B. W., and Bickford, M. E., 2013, Tectonic evolution of the Adirondack Mountains and
778 Grenville Orogen inliers within the USA: Geoscience Canada, v. 40, p. 318, doi:10.12789/geocanj.2013.40.022.
- 779 McMechan, M. E. and Price, R. A., 1982, Superimposed low-grade metamorphism in the Mount Fisher area,
780 southeastern British Columbia—implications for the East Kootenay orogeny: Canadian Journal of Earth
781 Sciences, v. 19, p. 476–489, doi:10.1139/e82-039.
- 782 Meert, J., der Voo, R. V., and Payne, T., 1994, Paleomagnetism of the Catoctin volcanic province: a new
783 Vendian-Cambrian apparent polar wander path for North America: Journal of Geophysical Research, v. 99, p.
784 4625–4641.
- 785 Meert, J. G. and Stuckey, W., 2002, Revisiting the paleomagnetism of the 1.476 Ga St. Francois Mountains igneous
786 province, Missouri: Tectonics, v. 21, doi:10.1029/2000tc001265.
- 787 Merdith, A. S., Collins, A. S., Williams, S. E., Pisarevsky, S., Foden, J. D., Archibald, D. B., Blades, M. L., Alessio,
788 B. L., Armistead, S., Plavsa, D., and et al., 2017, A full-plate global reconstruction of the Neoproterozoic:
789 Gondwana Research, v. 50, p. 84–134, doi:10.1016/j.gr.2017.04.001.
- 790 Met Office, 2010 - 2015, Cartopy: a cartographic python library with a matplotlib interface: Exeter, Devon, URL
791 <http://scitools.org.uk/cartopy>.
- 792 Middleton, R. S., Borradaile, G. J., Baker, D., and Lucas, K., 2004, Proterozoic diabase sills of northern Ontario:
793 Magnetic properties and history: Journal of Geophysical Research: Solid Earth, v. 109,
794 doi:10.1029/2003jb002581.
- 795 Mitchell, R. N., Bleeker, W., van Breemen, O., Lecheminant, T. N., Peng, P., Nilsson, M. K. M., and Evans, D.
796 A. D., 2014, Plate tectonics before 2.0 Ga: Evidence from paleomagnetism of cratons within supercontinent
797 Nuna: American Journal of Science, v. 314, p. 878–894, doi:10.2475/04.2014.03.
- 798 Mitchell, R. N., Hoffman, P. F., and Evans, D. A. D., 2010, Coronation loop resurrected: Oscillatory apparent polar
799 wander of orosirian (2.05–1.8†ga) paleomagnetic poles from slave craton: Precambrian Research, v. 179, p.
800 121–134.
- 801 Mitchell, R. N., Kilian, T. M., and Evans, D. A. D., 2012, Supercontinent cycles and the calculation of absolute
802 palaeolongitude in deep time: Nature, v. 482, p. 208–211, doi:10.1038/nature10800.
- 803 Müller, R. D., Cannon, J., Qin, X., Watson, R. J., Gurnis, M., Williams, S., Pfaffelmoser, T., Seton, M., Russell, S.
804 H. J., and Zahirovic, S., 2018, GPlates: Building a virtual earth through deep time: Geochemistry, Geophysics,
805 Geosystems, v. 19, p. 2243–2261, doi:10.1029/2018gc007584.

- 806 Murthy, G., Gower, C., Tubett, M., and Patzold, R., 1992, Paleomagnetism of Eocambrian Long Range dykes and
807 Double Mer Formation from Labrador, Canada: Canadian Journal of Earth Sciences, v. 29, p. 1224–1234,
808 doi:10.1139/e92-098.
- 809 Murthy, G. S., 1978, Paleomagnetic results from the Nain anorthosite and their tectonic implications: Canadian
810 Journal of Earth Sciences, v. 15, p. 516–525, doi:10.1139/e78-058.
- 811 Nesheim, T. O., Vervoort, J. D., McClelland, W. C., Gilotti, J. A., and Lang, H. M., 2012, Mesoproterozoic
812 syntectonic garnet within Belt Supergroup metamorphic tectonites: Evidence of Grenville-age metamorphism
813 and deformation along northwest Laurentia: Lithos, v. 134–135, p. 91–107, doi:10.1016/j.lithos.2011.12.008.
- 814 O'Neill, C., Lenardic, A., and Condie, K. C., 2013, Earth's punctuated tectonic evolution: cause and effect:
815 Geological Society, London, Special Publications, v. 389, p. 17–40, doi:10.1144/sp389.4.
- 816 Palin, R. M. and White, R. W., 2015, Emergence of blueschists on Earth linked to secular changes in oceanic crust
817 composition: Nature Geoscience, v. 9, p. 60–64, doi:10.1038/ngeo2605.
- 818 Palmer, H., 1970, Paleomagnetism and correlation of some Middle Keweenawan rocks, Lake Superior: Canadian
819 Journal of Earth Science, v. 7, p. 1410–1436, doi:10.1139/e70-136.
- 820 Palmer, H. C., Merz, B. A., and Hayatsu, A., 1977, The Sudbury dikes of the Grenville Front region:
821 paleomagnetism, petrochemistry, and K–Ar age studies: Canadian Journal of Earth Sciences, v. 14, p. 1867–1887.
- 822 Park, J. K., Irving, E., and Donaldson, J. A., 1973, Paleomagnetism of the Precambrian Dubawnt Group:
823 Geological Society of America Bulletin, v. 84, p. 859, doi:10.1130/0016-7606(1973)84<859:potpdg>2.0.co;2.
- 824 Pehrsson, S. J., Eglington, B. M., Evans, D. A. D., Huston, D., and Reddy, S. M., 2015, Metallogeny and its link to
825 orogenic style during the Nuna supercontinent cycle: Geological Society, London, Special Publications, v. 424,
826 doi:10.1144/SP424.5.
- 827 Pérez, F. and Granger, B. E., 2007, IPython: a system for interactive scientific computing: Computing in Science
828 and Engineering, v. 9, p. 21–29, doi:10.1109/MCSE.2007.53.
- 829 Pesonen, L., 1979, Paleomagnetism of late Precambrian Keweenawan igneous and baked contact rocks from
830 Thunder Bay district, northern Lake Superior: Bulletin of the Geological Society of Finland, v. 51, p. 27–44.
- 831 Pesonen, L. J. and Halls, H., 1979, The paleomagnetism of Keweenawan dikes from Baraga and Marquette
832 Counties, northern Michigan: Canadian Journal of Earth Science, v. 16, p. 2136–2149, doi:10.1139/e79-201.
- 833 Piispa, E. J., Smirnov, A. V., Pesonen, L. J., and Mitchell, R. H., 2018, Paleomagnetism and geochemistry of
834 1144-ma lamprophyre dikes, Northwestern Ontario: Implications for the North American polar wander and plate
835 velocities: Journal of Geophysical Research: Solid Earth, doi:10.1029/2018jb015992.

- 836 Piper, J., 1992, The palaeomagnetism of major (Middle Proterozoic) igneous complexes, South Greenland and the
837 Gardar apparent polar wander track: Precambrian Research, v. 54, p. 153 – 172,
838 doi:10.1016/0301-9268(92)90068-Y.
- 839 Piper, J. and Stearn, J., 1977, Palaeomagnetism of the dyke swarms of the Gardar Igneous Province, south
840 Greenland: Physics of the Earth and Planetary Interiors, v. 14, p. 345–358, doi:10.1016/0031-9201(77)90167-4.
- 841 Piper, J. D. A., 1977, Palaeomagnetism of the giant dykes of Tugtutoq and Narssaq Gabbro, Gardar Igneous
842 Province, South Greenland: Bull. Geol. Soc. Den, v. 26, p. 85–94.
- 843 Pisarevsky, S. A., Elming, S.-Å., Pesonen, L. J., and Li, Z.-X., 2014, Mesoproterozoic paleogeography:
844 Supercontinent and beyond: Precambrian Research, v. 244, p. 207–225, doi:10.1016/j.precamres.2013.05.014.
- 845 Pullaiah, G. and Irving, E., 1975, Paleomagnetism of the contact aureole and late dikes of the Otto stock, Ontario,
846 and its application to early proterozoic apparent polar wandering: Canadian Journal of Earth Sciences, v. 12, p.
847 1609–1618, doi:10.1139/e75-143.
- 848 Rapalini, A. E., 2018, The assembly of western Gondwana: Reconstruction based on paleomagnetic data: Geology
849 of Southwest Gondwana, p. 3–18, doi:10.1007/978-3-319-68920-3_1.
- 850 Redden, J., Peterman, Z., Zartman, R., and De-Witt, E., 1990, U-Th-Pb geochronology and preliminary
851 interpretation of Precambrian tectonic events in the Black Hills, South Dakota: *In* The Early Proterozoic
852 Trans-Hudson Orogen, Geological Association of Canada Special Paper 37, p. 229–251.
- 853 Rivers, T., 2008, Assembly and preservation of lower, mid, and upper orogenic crust in the Grenville
854 Province—implications for the evolution of large hot long-duration orogens: Precambrian Research, v. 167, p.
855 237–259, doi:10.1016/j.precamres.2008.08.005.
- 856 Robert, B., Besse, J., Blein, O., Greff-Lefftz, M., Baudin, T., Lopes, F., Meslouh, S., and Belbadaoui, M., 2017,
857 Constraints on the ediacaran inertial interchange true polar wander hypothesis: A new paleomagnetic study in
858 morocco (west african craton): Precambrian Research, v. 295, p. 90–116, doi:10.1016/j.precamres.2017.04.010.
- 859 Robertson, W. and Fahrig, W., 1971, The great Logan Loop - the polar wandering path from Canadian shield rocks
860 during the Neohelikian era: Canadian Journal of Earth Science, v. 8, p. 1355–1372, doi:10.1139/e71-125.
- 861 Roest, W. R. and Srivastava, S. P., 1989, Sea-floor spreading in the labrador sea: A new reconstruction: Geology,
862 v. 17, p. 1000, doi:10.1130/0091-7613(1989)017<1000:sfsitl>2.3.co;2.
- 863 Rooney, A. D., Austermann, J., Smith, E. F., Li, Y., Selby, D., Dehler, C. M., Schmitz, M. D., Karlstrom, K. E.,
864 and Macdonald, F. A., 2017, Coupled Re-Os and U-Pb geochronology of the Tonian Chuar Group, Grand
865 Canyon: GSA Bulletin, doi:10.1130/b31768.1.

- 866 Ross, G. M., 1991, Tectonic setting of the Windermere Supergroup revisited: Geology, v. 19, p. 1125,
867 doi:10.1130/0091-7613(1991)019<1125:tsotws>2.3.co;2.
- 868 Schmidt, P. W., 1980, Paleomagnetism of igneous rocks from the Belcher Islands, Northwest Territories, Canada:
869 Canadian Journal of Earth Sciences, v. 17, p. 807–822, doi:10.1139/e80-081.
- 870 Schulz, K. J. and Cannon, W. F., 2007, The Penokean orogeny in the Lake Superior region: Precambrian Research,
871 v. 157, p. 4–25, doi:10.1016/j.precamres.2007.02.022.
- 872 Schwarz, E. J., Clark, K. R., and Fujiwara, Y., 1982, Paleomagnetism of the Sutton Lake Proterozoic inlier,
873 Ontario, Canada: Canadian Journal of Earth Sciences, v. 19, p. 1330–1332, doi:10.1139/e82-114.
- 874 Selkin, P. A., Gee, J. S., Meurer, W. P., and Hemming, S. R., 2008, Paleointensity record from the 2.7 Ga Stillwater
875 Complex, Montana: Geochem. Geophys. Geosyst., v. 9, p. 10.1029/2008GC001,950.
- 876 Silver, P. G. and Behn, M. D., 2008, Intermittent plate tectonics?: Science, v. 319, p. 85–88.
- 877 Skipton, D. R., St-Onge, M. R., Schneider, D. A., and McFarlane, C. R. M., 2016, Tectonothermal evolution of the
878 middle crust in the Trans-Hudson Orogen, Baffin Island, Canada: Evidence from petrology and monazite
879 geochronology of sillimanite-bearing migmatites: Journal of Petrology, v. 57, p. 1437–1462,
880 doi:10.1093/petrology/egw046.
- 881 Slagstad, T., Culshaw, N. G., Daly, J. S., and Jamieson, R. A., 2009, Western Grenville Province holds key to
882 midcontinental Granite-Rhyolite Province enigma: Terra Nova, v. 21, p. 181–187,
883 doi:10.1111/j.1365-3121.2009.00871.x.
- 884 St-Onge, M. R., Van Gool, J. A. M., Garde, A. A., and Scott, D. J., 2009, Correlation of Archaean and
885 Palaeoproterozoic units between northeastern Canada and western Greenland: constraining the pre-collisional
886 upper plate accretionary history of the Trans-Hudson orogen: Geological Society, London, Special Publications,
887 v. 318, p. 193–235, doi:10.1144/sp318.7.
- 888 Stern, R. J. and Miller, N. R., 2018, Did the transition to plate tectonics cause neoproterozoic snowball earth?:
889 Terra Nova, v. 30, p. 87–94, doi:10.1111/ter.12321.
- 890 Stern, R. J., Tsujimori, T., Harlow, G., and Groat, L. A., 2013, Plate tectonic gemstones: Geology, v. 41, p.
891 723–726, doi:10.1130/g34204.1.
- 892 Swanson-Hysell, N. L., Burgess, S. D., Maloof, A. C., and Bowring, S. A., 2014a, Magmatic activity and plate
893 motion during the latent stage of Midcontinent Rift development: Geology, v. 42, p. 475–478,
894 doi:10.1130/G35271.1.
- 895 Swanson-Hysell, N. L., Ramezani, J., Fairchild, L. M., and Rose, I. R., 2019, Failed rifting and fast drifting:
896 Midcontinent Rift development, Laurentia's rapid motion and the driver of Grenvillian orogenesis: GSA Bulletin,
897 doi:10.1130/b31944.1.

- 898 Swanson-Hysell, N. L., Vaughan, A. A., Mustain, M. R., and Asp, K. E., 2014b, Confirmation of progressive plate
899 motion during the Midcontinent Rift's early magmatic stage from the Osler Volcanic Group, Ontario, Canada:
900 *Geochemistry Geophysics Geosystems*, v. 15, p. 2039–2047, doi:10.1002/2013GC005180.
- 901 Symons, D. and Chiasson, A., 1991, Paleomagnetism of the Callander Complex and the Cambrian apparent polar
902 wander path for North America: *Canadian Journal of Earth Science*, v. 1991, p. 355–363, doi:10.1139/e91-032.
- 903 Symons, D., Symons, T., and Lewchuk, M., 2000, Paleomagnetism of the Deschambault pegmatites: Stillstand and
904 hairpin at the end of the Paleoproterozoic Trans-Hudson Orogeny, Canada: *Physics and Chemistry of the Earth*,
905 Part A: Solid Earth and Geodesy, v. 25, p. 479–487, doi:10.1016/s1464-1895(00)00074-0.
- 906 Symons, D. T. A. and Mackay, C. D., 1999, Paleomagnetism of the Boot-Phantom pluton and the amalgamation of
907 the juvenile domains in the Paleoproterozoic Trans-Hudson Orogen, Canada: In Sinha, A. K., ed., *Basement*
908 *Tectonics* 13, Springer Netherlands, Dordrecht, p. 313–331, doi:10.1007/978-94-011-4800-9{_}18.
- 909 Tanczyk, E., Lapointe, P., Morris, W., and Schmidt, P., 1987, A paleomagnetic study of the layered mafic intrusions
910 at Sept-Iles, Quebec: *Canadian Journal of Earth Science*, v. 24, p. 1431–1438, doi:10.1139/e87-135.
- 911 Tauxe, L. and Kodama, K., 2009, Paleosecular variation models for ancient times: Clues from Keweenawan lava
912 flows: *Physics of the Earth and Planetary Interiors*, v. 177, p. 31–45, doi:10.1016/j.pepi.2009.07.006.
- 913 Tauxe, L., Shaar, R., Jonestrask, L., Swanson-Hysell, N., Minnett, R., Koppers, A., Constable, C., Jarboe, N.,
914 Gaastra, K., and Fairchild, L., 2016, PmagPy: Software package for paleomagnetic data analysis and a bridge to
915 the Magnetics Information Consortium (MagIC) Database: *Geochemistry, Geophysics, Geosystems*,
916 doi:10.1002/2016GC006307.
- 917 Torsvik, T. H. and Cocks, L. R. M., 2017, Earth history and palaeogeography: Cambridge University Press,
918 doi:10.1017/9781316225523.
- 919 Torsvik, T. H., van der Voo, R., Doubrovine, P. V., Burke, K., Steinberger, B., Ashwal, L. D., Trønnes, R. G.,
920 Webb, S. J., and Bull, A. L., 2014, Deep mantle structure as a reference frame for movements in and on the
921 Earth: *Proceedings of the National Academy of Sciences*, doi:10.1073/pnas.1318135111.
- 922 Torsvik, T. H., Van der Voo, R., Preeden, U., Mac Niocaill, C., Steinberger, B., Doubrovine, P. V., van Hinsbergen,
923 D. J. J., Domeier, M., Gaina, C., Tohver, E., Meert, J. G., McCausland, P. J. A., and Cocks, L. R. M., 2012,
924 Phanerozoic polar wander, palaeogeography and dynamics: *Earth-Science Reviews*, v. 114, p. 325–368,
925 doi:10.1016/j.earscirev.2012.06.007.
- 926 Veikkolainen, T., Pesonen, L., and Evans, D. D., 2014, PALEOMAGIA: A PHP/MYSQL database of the
927 Precambrian paleomagnetic data: p. 1–17, doi:10.1007/s11200-013-0382-0.

- 928 Warnock, A., Kodama, K., and Zeitler, P., 2000, Using thermochronometry and low-temperature demagnetization
 929 to accurately date Precambrian paleomagnetic poles: *Journal of Geophysical Research*, v. 105, p. 19,435–19,453,
 930 doi:10.1029/2000jb900114.
- 931 Weil, A., Geissman, J., Heizler, M., and Van der Voo, R., 2003, Paleomagnetism of Middle Proterozoic mafic
 932 intrusions and Upper Proterozoic (Nankoweap) red beds from the Lower Grand Canyon Supergroup, Arizona:
 933 *Tectonophysics*, v. 375, p. 199–220, doi:10.1016/S0040-1951(03)00339-1.
- 934 Weil, A. B., Geissman, J. W., and Ashby, J. M., 2006, A new paleomagnetic pole for the Neoproterozoic Uinta
 935 Mountain supergroup, Central Rocky Mountain States, USA: *Precambrian Research*, v. 147, p. 234–259,
 936 doi:10.1016/j.precamres.2006.01.017.
- 937 Weil, A. B., Geissman, J. W., and Voo, R. V. d., 2004, Paleomagnetism of the Neoproterozoic Chuar Group, Grand
 938 Canyon Supergroup, Arizona: implications for Laurentia's Neoproterozoic APWP and Rodinia break-up:
 939 *Precambrian Research*, v. 129, p. 71–92.
- 940 Weller, O. M. and St-Onge, M. R., 2017, Record of modern-style plate tectonics in the Palaeoproterozoic
 941 Trans-Hudson orogen: *Nature Geoscience*, v. 10, doi:10.1038/ngeo2904.
- 942 Whitmeyer, S. and Karlstrom, K., 2007, Tectonic model for the Proterozoic growth of North America: *Geosphere*,
 943 v. 3, p. 220–259, doi:10.1130/GES00055.1.
- 944 Witkosky, R. and Wernicke, B. P., 2018, Subsidence history of the Ediacaran Johnnie Formation and related strata
 945 of southwest Laurentia: Implications for the age and duration of the Shuram isotopic excursion and animal
 946 evolution: *Geosphere*, v. 14, p. 2245–2276, doi:10.1130/ges01678.1.
- 947 Zhang, S., Li, Z.-X., Evans, D. A. D., Wu, H., Li, H., and Dong, J., 2012, Pre-Rodinia supercontinent Nuna shaping
 948 up: A global synthesis with new paleomagnetic results from North China: *Earth and Planetary Science Letters*,
 949 v. 353–354, p. 145–155.

Table 1. Rotations of separated terranes

Block	Euler pole longitude	Euler pole latitude	rotation angle	note and citation
Greenland	-118.5	67.5	-13.8	Cenozoic separation of Greenland from Laurentia associated with opening of Baffin Bay and the Labrador Sea (Roest and Srivastava, 1989)
Scotland	161.9	78.6	-31.0	Reconstructing Atlantic opening following Torsvik and Cocks (2017)
Svalbard	125.0	-81.0	68	Rotate Svalbard to Laurentia in fit that works well with East Greenland basin according to Maloof et al. (2006)

Table 2: Compilation of paleomagnetic poles from Laurentia

terrane	unit name	Nordic rating	site lon (°)	site lat (°)	plon (°)	plat (°)	A ₉₅ (°)	age (Ma)	pole reference
Laurentia-	Stillwater Complex	A	249.2	45.2	335.8	-83.6	4.0	2705 ⁺⁴ ₋₄	Selkin et al. (2008)
Wyoming	- C2								
Laurentia-	Otto Stock dykes	B	279.9	48.0	227.0	69.0	4.8	2676 ⁺⁵ ₋₅	Pullaiah and Irving (1975)
Superior(East)	and aureole								
Laurentia-Slave	Defeat Suite	B	245.5	62.5	64.0	-1.0	15.0	2625 ⁺⁵ ₋₅	Mitchell et al. (2014)
Laurentia-	Ptarmigan-	B	287.0	54.0	213.0	-45.3	13.8	2505 ⁺² ₋₂	Evans and Halls (2010)
Superior(East)	Mistassini dykes								
Laurentia-	Matachewan dykes	A	278.0	48.0	238.3	-44.1	1.6	2466 ⁺²³ ₋₂₃	Evans and Halls (2010)
Superior(East)	R								
Laurentia-	Matachewan dykes	A	278.0	48.0	239.5	-52.3	2.4	2446 ⁺³ ₋₃	Evans and Halls (2010)
Superior(East)	N								
Laurentia-Slave	Malley dykes	A	249.8	64.2	310.0	-50.8	6.7	2231 ⁺² ₋₂	Buchan et al. (2012)
Laurentia-	Senneterre dykes	A	283.0	49.0	284.3	-15.3	5.5	2218 ⁺⁶ ₋₆	Buchan et al. (1993)
Superior(East)									
Laurentia-	Nipissing N1 sills	A	279.0	47.0	272.0	-17.0	10.0	2217 ⁺⁴ ₋₄	Buchan et al. (2000)
Superior(East)									
Laurentia-Slave	Dogrib dykes	A	245.5	62.5	315.0	-31.0	7.0	2193 ⁺² ₋₂	Mitchell et al. (2014)
Laurentia-	Biscotasing dykes	A	280.0	48.0	223.9	26.0	7.0	2170 ⁺³ ₋₃	Evans and Halls (2010)
Superior(East)									
Laurentia-	Rabbit Creek,	A	252.8	43.9	339.2	65.5	7.6	2160 ⁺¹¹ ₋₈	Kilian et al. (2015)
Wyoming	Powder River and								
	South Path Dykes								
Laurentia-Slave	Indin dykes	A	245.6	62.5	256.0	-36.0	7.0	2126 ⁺³ ₋₁₈	Buchan et al. (2016)
Laurentia-	Marathon dykes N	A	275.0	49.0	198.2	45.4	7.7	2124 ⁺³ ₋₃	Halls et al. (2008)
Superior(West)									

Continued on next page

terrane	unit name	Nordic rating	site lon (°)	site lat (°)	plon (°)	plat (°)	A ₉₅ (°)	age (Ma)	pole reference
Laurentia-Superior(West)	Marathon dykes R	A	275.0	49.0	182.2	55.1	7.5	2104 ⁺³ ₋₃	Halls et al. (2008)
Laurentia-Superior(West)	Cauchon Lake dykes	A	263.0	56.0	180.9	53.8	7.7	2091 ⁺² ₋₂	Evans and Halls (2010)
Laurentia-Superior(West)	Fort Frances dykes	A	266.0	48.0	184.6	42.8	6.1	2077 ⁺⁵ ₋₅	Evans and Halls (2010)
Laurentia-Superior(East)	Lac Esprit dykes	A	282.0	53.0	170.5	62.0	6.4	2069 ⁺¹ ₋₁	Evans and Halls (2010)
Laurentia-Greenland-Nain	Kangamiut Dykes	B	307.0	66.0	273.8	17.1	2.7	2042 ⁺¹² ₋₁₂	Fahrig and Bridgwater (1976)
Laurentia-Slave	Lac de Gras dykes	A	249.6	64.4	267.9	11.8	7.1	2026 ⁺⁵ ₋₅	Buchan et al. (2009)
Laurentia-Superior(East)	Minto dykes	A	285.0	57.0	171.5	38.7	13.1	1998 ⁺² ₋₂	Evans and Halls (2010)
Laurentia-Slave	Rifle Formation	B	252.9	65.9	341.0	14.0	7.7	1963 ⁺⁶ ₋₆	Evans and Hoye (1981)
Laurentia-Rae	Clearwater Anorthosite	B	251.6	57.1	311.8	6.5	2.9	1917 ⁺⁷ ₋₇	Halls and Hanes (1999)
Laurentia-Wyoming	Sourdough mafic dike swarm	A	-108.3	44.7	292.0	49.2	8.1	1899 ⁺⁵ ₋₅	Kilian et al. (2016)
Laurentia-Slave	Ghost Dike Swarm	A	244.6	62.6	286.0	-2.0	6.0	1887 ⁺⁵ ₋₉	Buchan et al. (2016)
Laurentia-Slave	Mean Se-ton/Akaitcho/Mara	B	250.0	65.0	260.0	-6.0	4.0	1885 ⁺⁵ ₋₅	Mitchell et al. (2010)
Laurentia-Slave	Mean Kahochella, Peacock Hills	B	250.0	65.0	285.0	-12.0	7.0	1882 ⁺⁴ ₋₄	Mitchell et al. (2010)
Laurentia-Superior(West)	Molson (B+C2) dykes	A	262.0	55.0	218.0	28.9	3.8	1879 ⁺⁶ ₋₆	Evans and Halls (2010)

Continued on next page

terrane	unit name	Nordic rating	site lon (°)	site lat (°)	plon (°)	plat (°)	A ₉₅ (°)	age (Ma)	pole reference
Laurentia-Slave	Douglas Peninsula Formation, Pethei Group	B	249.7	62.8	258.0	-18.0	14.2	1876 ⁺¹⁰ ₋₁₀	Irving and McGlynn (1979)
Laurentia-Slave	Takiyuak Formation	B	246.9	66.1	249.0	-13.0	8.0	1876 ⁺¹⁰ ₋₁₀	Irving and McGlynn (1979)
Laurentia-Superior	Haig/Flaherty/Sutton Mean	B	279.0	56.0	245.8	1.0	3.9	1870 ⁺¹ ₋₁	Nordic workshop calculation based on data of Schmidt (1980); Schwarz et al. (1982)
Laurentia-Slave	Pearson A/Peninsular/Kilohigok sills	A	250.0	65.0	269.0	-22.0	6.0	1870 ⁺⁴ ₋₄	Mitchell et al. (2010)
Laurentia-Trans-Hudson orogen	Boot-Phantom Pluton	B	258.1	54.7	275.4	62.4	7.9	1838 ⁺¹ ₋₁	Symons and Mackay (1999)
Laurentia-Rae	Sparrow Dykes	B	250.2	61.6	291.0	12.0	7.9	1827 ⁺⁴ ₋₄	McGlynn et al. (1974)
Laurentia-Rae	Martin Formation	A	251.4	59.6	288.0	-9.0	8.5	1818 ⁺⁴ ₋₄	Evans and Bingham (1973)
Laurentia	Dubawnt Group	B	265.6	64.1	277.0	7.0	8.0	1785 ⁺³⁵ ₋₃₅	Park et al. (1973)
Laurentia-Trans-Hudson orogen	Deschambault Pegmatites	B	256.7	54.9	276.0	67.5	7.7	1766 ⁺⁵ ₋₅	Symons et al. (2000)
Laurentia-Trans-Hudson orogen	Jan Lake Granite	B	257.2	54.9	264.3	24.3	16.9	1758 ⁺¹ ₋₁	Gala et al. (1995)
Laurentia	Cleaver Dykes	A	242.0	67.5	276.7	19.4	6.1	1741 ⁺⁵ ₋₅	Irving (2004)
Laurentia-Greenland	Melville Bugt dia-base dykes	B	303.0	74.6	273.8	5.0	8.7	1633 ⁺⁵ ₋₅	Halls et al. (2011)
Laurentia	Western Channel Diabase	A	242.2	66.4	245.0	9.0	6.6	1590 ⁺³ ₋₃	Irving and Park (1972)

Continued on next page

terrane	unit name	Nordic rating	site lon (°)	site lat (°)	plon (°)	plat (°)	A ₉₅ (°)	age (Ma)	pole reference
Laurentia	St.Francois Mountains Acidic Rocks	A	269.5	37.5	219.0	-13.2	6.1	1476 ⁺¹⁶ ₋₁₆	Meert and Stuckey (2002)
Laurentia	Michikamau Intrusion	A	296.0	54.5	217.5	-1.5	4.7	1460 ⁺⁵ ₋₅	Emslie et al. (1976)
Laurentia	Spokane Formation	A	246.8	48.2	215.5	-24.8	4.7	1458 ⁺¹³ ₋₁₃	Elston et al. (2002)
Laurentia	Snowslip Formation	A	245.9	47.9	210.2	-24.9	3.5	1450 ⁺¹⁴ ₋₁₄	Elston et al. (2002)
Laurentia	Tobacco Root dykes	B	247.6	47.4	216.1	8.7	10.5	1448 ⁺⁴⁹ ₋₄₉	Harlan et al. (2008)
Laurentia	Purcell Lava	A	245.1	49.4	215.6	-23.6	4.8	1443 ⁺⁷ ₋₇	Elston et al. (2002)
Laurentia	Rocky Mountain intrusions	B	253.8	40.3	217.4	-11.9	9.7	1430 ⁺¹⁵ ₋₁₅	Nordic workshop calculation based on data of Harlan et al. (1994); Harlan and Geissman (1998)
Laurentia	Mistastin Pluton	B	296.3	55.6	201.5	-1.0	7.6	1425 ⁺²⁵ ₋₂₅	Fahrig and Jones (1976)
Laurentia	McNamara Formation	A	246.4	46.9	208.3	-13.5	6.7	1401 ⁺⁶ ₋₆	Elston et al. (2002)
Laurentia	Pilcher, Garnet Range and Libby Formations	A	246.4	46.7	215.3	-19.2	7.7	1385 ⁺²³ ₋₂₃	Elston et al. (2002)
Laurentia-Greenland	Zig-Zag Dal Basalts	B	334.8	81.2	242.8	12.0	3.8	1382 ⁺² ₋₂	Marcussen and Abrahamsen (1983)
Laurentia-Greenland	Midsommersoe Dolerite	B	333.4	81.6	242.0	6.9	5.1	1382 ⁺² ₋₂	Marcussen and Abrahamsen (1983)
Laurentia-Greenland	Victoria Fjord dolerite dykes	B	315.3	81.5	231.7	10.3	4.3	1382 ⁺² ₋₂	Abrahamsen and Van Der Voo (1987)

Continued on next page

terrane	unit name	Nordic rating	site lon (°)	site lat (°)	plon (°)	plat (°)	A_{95} (°)	age (Ma)	pole reference
Laurentia	Nain Anorthosite	B	298.2	56.5	206.7	11.7	2.2	1305^{+15}_{-15}	Murthy (1978)
Laurentia-Greenland	North Qoroq intrusives	B	314.6	61.1	202.6	13.2	8.3	1275^{+1}_{-1}	Piper (1992)
Laurentia-Greenland	Kungnat Ring Dyke	B	311.7	61.2	198.7	3.4	3.2	1275^{+2}_{-2}	Piper and Stearn (1977)
Laurentia	Mackenzie dykes	A	250.0	65.0	190.0	4.0	5.0	1267^{+2}_{-2}	Buchan et al. (2000)
	grand mean								
Laurentia-Greenland	West Gardar Dolerite Dykes	B	311.7	61.2	201.7	8.7	6.6	1244^{+8}_{-8}	Piper and Stearn (1977)
Laurentia-Greenland	West Gardar Lamprophyre Dykes	B	311.7	61.2	206.4	3.2	7.2	1238^{+11}_{-11}	Piper and Stearn (1977)
Laurentia	Sudbury Dykes	A	278.6	46.3	192.8	-2.5	2.5	1237^{+5}_{-5}	Palmer et al. (1977)
	Combined								
Laurentia-Scotland	Stoer Group	B	354.5	58.0	238.4	37.2	7.7	1199^{+70}_{-70}	Nordic workshop calculation
Laurentia-Greenland	Narssaq Gabbro	B	313.8	60.9	225.4	31.6	9.7	1184^{+5}_{-5}	Piper (1977)
Laurentia-Greenland	Hviddal Giant Dyke	B	313.7	60.9	215.3	33.2	9.6	1184^{+5}_{-5}	Piper (1977)
Laurentia-Greenland	South Qoroq Intr.	A	314.6	61.1	215.9	41.8	13.1	1163^{+2}_{-2}	Piper (1992)
Laurentia-Greenland	Giant Gabbro Dykes	B	313.7	60.9	226.1	42.3	9.4	1163^{+2}_{-2}	Piper (1977)
Laurentia-Greenland	NE-SW Trending dykes	B	314.6	61.1	230.8	33.4	5.7	1160^{+5}_{-5}	Piper (1992)
Laurentia	Ontario lamprophyre dykes	NR	273.3	48.8	223.3	58.0	9.2	1143^{+10}_{-10}	Piispa et al. (2018)

Continued on next page

terrane	unit name	Nordic rating	site lon (°)	site lat (°)	plon (°)	plat (°)	A_{95} (°)	age (Ma)	pole reference
Laurentia	Abitibi Dykes	A	279.0	48.0	215.5	48.8	14.1	1141^{+2}_{-2}	Ernst and Buchan (1993)
Laurentia	Nipigon sills and lavas	A	270.9	49.1	217.8	47.2	4.0	1109^{+2}_{-2}	Nordic workshop calculation based on data of Palmer (1970); Robertson and Fahrig (1971); Pesonen (1979); Pesonen and Halls (1979); Middleton et al. (2004); Borradaile and Middleton (2006)
Laurentia	Lowermost Mamainse Point volcanics -R1	A	275.3	47.1	227.0	49.5	5.3	1109^{+2}_{-3}	Swanson-Hysell et al. (2014a)
Laurentia	Lower Osler volcanics -R	A	272.3	48.8	218.6	40.9	4.8	1108^{+3}_{-3}	Swanson-Hysell et al. (2014b)
Laurentia	Middle Osler volcanics -R	A	272.4	48.8	211.3	42.7	8.2	1107^{+4}_{-4}	Swanson-Hysell et al. (2014b)
Laurentia	Upper Osler volcanics -R	A	272.4	48.7	203.4	42.3	3.7	1105^{+1}_{-1}	Halls (1974); Swanson-Hysell et al. (2014b, 2019)
Laurentia	Lower Mamainse Point volcanics -R2	A	275.3	47.1	205.2	37.5	4.5	1105^{+3}_{-4}	Swanson-Hysell et al. (2014a)
Laurentia	Mamainse Point volcanics -C (lower N, upper R)	A	275.3	47.1	189.7	36.1	4.9	1101^{+1}_{-1}	Swanson-Hysell et al. (2014a)
Laurentia	North Shore lavas -N	A	268.7	46.3	181.7	31.1	2.1	1097^{+3}_{-3}	Tauxe and Kodama (2009); Swanson-Hysell et al. (2019)

Continued on next page

terrane	unit name	Nordic rating	site lon (°)	site lat (°)	plon (°)	plat (°)	A ₉₅ (°)	age (Ma)	pole reference
Laurentia	Portage Lake Volcanics	A	271.2	47.0	182.5	27.5	2.3	1095 ₋₃ ⁺³	Books (1972); Hnat et al. (2006) as calculated in Swanson-Hysell et al. (2019)
Laurentia	Chengwatana Volcanics	B	267.3	45.4	186.1	30.9	8.2	1095 ₋₂ ⁺²	Kean et al. (1997)
Laurentia	Uppermost Mainse Point volcanics -N	A	275.3	47.1	183.2	31.2	2.5	1094 ₋₄ ⁺⁶	Swanson-Hysell et al. (2014a)
Laurentia	Cardenas Basalts and Intrusions	B	248.1	36.1	185.0	32.0	8.0	1091 ₋₅ ⁺⁵	Weil et al. (2003)
Laurentia	Schroeder Lutsen Basalts	A	269.1	47.5	187.8	27.1	3.0	1090 ₋₇ ⁺²	Fairchild et al. (2017)
Laurentia	Central Arizona diabases -N	A	249.2	33.7	175.3	15.7	7.0	1088 ₋₁₁ ⁺¹¹	Donadini et al. (2011)
Laurentia	Lake Shore Traps	A	271.9	47.6	186.4	23.1	4.0	1086 ₋₁ ⁺¹	Kulakov et al. (2013)
Laurentia	Michipicoten Island Formation	A	274.3	47.7	174.7	17.0	4.4	1084 ₋₁ ⁺¹	Fairchild et al. (2017)
Laurentia	Nonesuch Shale	B	271.5	47.0	178.1	7.6	5.5	1080 ₋₁₀ ⁺⁴	Henry et al. (1977)
Laurentia	Freda Sandstone	B	271.5	47.0	179.0	2.2	4.2	1070 ₋₁₀ ⁺¹⁴	Henry et al. (1977)
Laurentia	Haliburton Intrusions	B	281.4	45.0	141.9	-32.6	6.3	1015 ₋₁₅ ⁺¹⁵	Warnock et al. (2000)
Laurentia-Scotland	Torridon Group	B	354.3	57.9	220.9	-17.7	7.1	925 ₋₁₄₅ ⁺¹⁴⁵	Nordic workshop calculation
Laurentia-Svalbard	Lower Grusdievbreen Formation	B	18.0	79.0	204.9	19.6	10.9	831 ₋₂₀ ⁺²⁰	Maloof et al. (2006)

Continued on next page

terrane	unit name	Nordic rating	site lon (°)	site lat (°)	plon (°)	plat (°)	A ₉₅ (°)	age (Ma)	pole reference
Laurentia-Svalbard	Upper Grus-dievbreen Formation	B	18.2	78.9	252.6	-1.1	6.2	800 ⁺¹¹ ₋₁₁	Maloof et al. (2006)
Laurentia	Gunbarrel dykes	B	248.7	44.8	138.2	9.1	12.0	778 ⁺² ₋₂	Calculation from Eyster et al. (2019) based on data of Harlan (1993); Harlan et al. (1997)
Laurentia-Svalbard	Svanbergfjellet Formation	B	18.0	78.5	226.8	25.9	5.8	770 ⁺¹⁹ ₋₄₀	Maloof et al. (2006)
Laurentia	Uinta Mountain Group	B	250.7	40.8	161.3	0.8	4.7	760 ⁺⁶ ₋₁₀	Weil et al. (2006)
Laurentia	Carbon Canyon	NR	248.2	36.1	166.0	-0.5	9.7	757 ⁺⁷ ₋₇	Weil et al. (2004) as calculated in Eyster et al. (2019)
Laurentia	Carbon Butte/Awatubi	NR	248.5	35.2	163.8	14.2	3.5	751 ⁺⁸ ₋₈	Eyster et al. (2019)
Laurentia	Franklin event grand mean	A	275.4	73.0	162.1	6.7	3.0	724 ⁺³ ₋₃	Denyszyn et al. (2009a)
Laurentia	Long Range Dykes	B	303.3	53.7	355.3	19.0	17.4	615 ⁺² ₋₂	Murthy et al. (1992)
Laurentia	Baie des Moutons complex	B	301.0	50.8	321.5	-34.2	15.4	583 ⁺² ₋₂	McCausland et al. (2011)
Laurentia	Baie des Moutons complex	B	301.0	50.8	332.7	42.6	12.0	583 ⁺² ₋₂	McCausland et al. (2011)
Laurentia	Callander Alkaline Complex	B	280.6	46.2	301.4	46.3	6.0	575 ⁺⁵ ₋₅	Symons and Chiasson (1991)
Laurentia	Catoctin Basalts	B	281.8	38.5	296.7	42.0	17.5	572 ⁺⁵ ₋₅	Meert et al. (1994)

Continued on next page

terrane	unit name	Nordic rating	site lon (°)	site lat (°)	plon (°)	plat (°)	A ₉₅ (°)	age (Ma)	pole reference
Laurentia	Sept-Iles layered intrusion	B	293.5	50.2	321.0	-20.0	6.7	565 ⁺⁴ ₋₄	Tanczyk et al. (1987)